Revisiting global hydrological cycle: Is it intensifying?

Demetris Koutsoyiannis

Department of Water Resources and Environmental Engineering, School of Civil Engineering, National Technical University of Athens, Heroon Polytechneiou 5, GR 157 80 Zographou, Greece

5   *Correspondence to: dk@itia.ntua.gr*

Abstract. As a result of technological advances in monitoring atmosphere, hydrosphere, cryosphere and biosphere, as well as in data management and processing, several data bases have become freely available. These can be exploited in revisiting the global hydrological cycle with the aim, on the one hand, to better quantify it and, on the other hand, to test the established climatological hypotheses, according to which the hydrological cycle should be intensifying because of global warming. By
10   processing the information from gridded ground observations, satellite data and reanalyses, it turns out that the established hypotheses are not confirmed. Instead of monotonic trends, there appear fluctuations from intensification to deintensification and vice versa, with deintensification prevailing in the 21st century. The water balance on land and sea appears to be lower than the standard figures of literature, but with greater variability on climatic time scales, which is in accordance with Hurst-Kolmogorov stochastic dynamics. The most obvious anthropogenic signal in the hydrological cycle appears to be the
15   overexploitation of groundwater, which has a visible effect on sea level rise. Melting of glaciers has an equal effect, but in this case it is not known which part is anthropogenic, as studies on polar regions attribute mass loss mostly to ice dynamics.

> *«Πεπαιδευμένου γάρ ἐστιν ἐπὶ τοσοῦτον τἀκριβὲς ἐπιζητεῖν καθ᾽ ἕκαστον γένος, ἐφ᾽ ὅσον ἡ τοῦ πράγματος φύσις ἐπιδέχεται»*
> ("*It is the mark of an educated man to look for precision in each class of things just so far as the nature of the subject admits*")
> Aristotle, Nicomachean Ethics, 1094b.

1   Introduction

If the dark side of concerns about earth's climate is *scare*, the bright side is *data*. The latter single-word label means to include the technological advances in monitoring atmosphere, hydrosphere, cryosphere and biosphere, the gathering and processing of huge amounts of ground- and space-based observations for the land and sea parts of the earth, and the free availability of data. Hydrological processes on the global scale extend over all these spheres and our knowledge of them is benefited from
25   these data.

The availability of different types of data allows revisiting the global hydrological cycle and improving its own quantified knowledge. It can also be useful in testing the climatological hypotheses that are relevant to hydrology. Among them, crucial is the conjecture that, in a warming climate, atmospheric moisture is changing in a manner that the relative humidity remains constant, but specific humidity increases according to the Clausius–Clapeyron relationship. As a result, the established view

30 is that the global atmospheric water vapour should increase by about 6%–7% per °C of warming. This gives rise to what has been called intensification of hydrological cycle. Because of the alleged intensification, the role of hydrology becomes thus important in the climate agenda from a sociological point of view: some of the most prominent predicted catastrophes are related to water shortage and extreme floods (Koutsoyiannis, 2014a).

Hence, the purpose of this study is to revisit the hydrological cycle in an era of climate change concerns and rich data
35 availability with an emphasis in the following points:

1. Overviewing and retrieving a great amount of global hydroclimatic datasets.
2. Improving the quantification of the global hydrological cycle, its variability and its uncertainties, through the surge of newly available data sets.
3. Testing established climatological hypotheses, according to which the hydrological cycle should be intensifying
40 because of global warming.
4. Outlining a stochastic view of hydroclimate which provides reliable means to deal with its variability.

These points are reflected in the structure of the paper in the following manner. The material related to point 1 is detailed in section 2. Sections 3 to 5 are aligned according to point 2, the quantification of the global hydrological cycle. On the other hand, point 3 elevates the significance of atmospheric water and, thus, section 3 is devoted to this. Precipitation and evaporation
45 are the key components of the hydrological cycle whose imbalance in the land part of earth drives all other hydrological processes. Quantification and changes in these drivers are examined in section 4. Based on the results in section 4, the water balance per se is studied in section 5. Morever, to quantify storage changes within water balance, and in particular the groundwater and cryosphere storage changes, section 5 includes an extended review of related literature.

Point 3 is dealt with, together with point 2, in sections 3 and 4, devoted to the atmospheric water, precipitation and
50 evaporation, as well as in two Appendices, which provide additional information on testing established climatological hypotheses. Point 4 is contained in section 6, whose scope is the future hydroclimatic variability. The necessity of proposing a stochastic approach to hydroclimate becomes obvious after examining whether climate models (and other more empirical techniques commonly used) are consistent with the reality (tracked in the earlier sections) and skilful, so as to be usable for future hydrological projections. It turns out that the state of affairs with current common methodologies is not satisfactory and
55 hence the need for an alternative approach emerges. This has to be stochastic and consistent with observed natural behaviours, as outlined in section 6. Finally, section 7 concludes the study with relevant remarks.

2 Data sets and processing

2.1 Sources of information

This study tries to use a wide range of available data sets reflecting the real-world hydrological cycle at the global level, either
60 directly (by accessing the data per se) or indirectly (by using processed data and results from other studies). In particular, the

information used comprises: (a) gridded ground observations, (b) satellite data and (c) reanalysis data. Gridded ground observations are available for precipitation over land. Gridded satellite data exist for several variables of hydrologic importance including air temperature, water vapour amount, cloud water amount, precipitation and snow cover, as detailed in the next subsections. Information from reanalyses is far richer, as these provide numerical description of the weather system in terms
65   of a great deal of atmospheric variables by combining numerical weather prediction models with observations. Here we use NCEP-NCAR and ERA5 reanalyses, which are publicly available.

The NCEP-NCAR Reanalysis 1 (Kalnay et al., 1996) is jointly produced by the National Center for Environmental Prediction (NCEP) and the National Center for Atmospheric Research (NCAR). Its temporal coverage includes 4-times daily, daily and monthly values for 1948 to present at a horizontal resolution of 1.88° (~ 210 km). It uses a state-of-the-art
70   analysis/forecast system to perform data assimilation using observations and a numerical weather prediction model. The data assimilation and the model used are identical to the global system implemented operationally at NCEP except in the horizontal resolution. A large subset of these data is available as daily and monthly averages.

The ERA5 (Copernicus Climate Change Service, 2017) is the fifth-generation atmospheric reanalysis of the European Centre for Medium-Range Weather Forecasts (ECMWF), where the name ERA refers to *ECMWF ReAnalysis*. It spans the
75   modern observing period from 1979 onward, with daily updates continuing forward in time, with fields available at a horizontal resolution of 31 km on 139 levels, from the surface up to 0.01 hPa (around 80 km). It has been produced as an operational service and its fields compare well with the ECMWF operational analyses (Hersbach and Dee, 2016).

We did not use the longer-term reanalyses that appeared recently to serve climate change studies as these have lower reliability. Specifically, the ERA-20C reanalysis which covers the period 1900-2010, compares poorly even to the ERA5
80   reanalysis, developed by the same institution (ECMWF), while the 20CR V3 reanalysis (the Twentieth Century Reanalysis V3 by NOAA-CIRES-DOE), which covers the period 1836-2015 has, in addition, huge departures in the precipitation and evaporation quantities over the globe, with the global imbalance being more than half of the precipitation over land or almost twice the runoff. Therefore, here they are judged as not hydrologically useful.

In addition, this study uses results from several other studies which are based on different data sets, such as GRACE
85   (Gravity Recovery and Climate Experiment; Syed et al., 2009; Eicker et al., 2016; Schellekens et al., 2017); LDAS (NASA's Global Land Data Assimilation System; Zhou et al., 2019), and hydrological models such as GRUN (global gridded monthly reconstruction of runoff, 1902 – 2014; Ghiggi et al., 2019) or PCR-GLOBWB (Wada et al., 2010), which stands for *PC Raster Global Water Balance*. Archfield et al. (2015) provide additional links for other useful data sources.

In the next subsections we describe each data set used, while in Table 1 we summarize all details and provide all
90   necessary links to the retrieved information, so that the user can easily reproduce the results of this study. In general, we use actual values of time series, disfavouring the popular notion of "anomalies", i.e. for differences from a certain mean[*], which

---

[*] *Anomaly*, originally *ανωμαλία*, is the Greek word for *abnormality*. As the departure from the mean is *the* normal behaviour in all undead systems, the name is clearly a terrible misnomer for the aimed meaning. For this reason, here, when we refer to data series originally designated as such, we use quotation marks.

have only a statistical, rather than a physical, meaning, while, even in a statistical context, they have several disadvantages (e.g. they hide biases). Thus, whenever possible, data originally given as "anomalies" are converted here to actual values. As usually the "anomalies" are taken from monthly means, by converting them to actual values we reinstate the seasonality. For this reason, the information given in this study in terms of graphs differs substantially from familiar graphs of the climatic literature. This is a deliberate choice in an attempt not to hide variability. All graphs also include running averages on the annual scale and thus the temporal mean and variability on annual and multiyear scales are also highlighted in the graphs.

2.2   Temperature and dew point data

The satellite temperature dataset, developed at the University of Alabama in Huntsville (UAH), infers the temperature, T, of three broad levels of the atmosphere from satellite measurements of the oxygen radiance in the microwave band, using advanced (passive) microwave sounding units on NOAA and NASA satellites (Spencer and Christy, 1990; Christy et al., 2007). The data are publicly available on monthly scale in the forms of time series of "anomalies" for several parts of earth, as well as in maps. Here we use only the global average on monthly scale for the lowest level, referred to as the lower troposphere, after conversion of "anomalies" to actual temperatures.

For the more recent years, monthly land surface temperature and emissivity are also available from the Moderate Resolution Imaging Spectroradiometer (MODIS), a key instrument aboard two satellites: the Terra (originally known as EOS AM-1) and the Aqua (originally known as EOS PM-1), providing observations since 2000 and 2002, respectively. The MOD11C3 Version 6 product provides temperature values on a 0.05° grid, which are derived by compositing and averaging the values from the corresponding month of MOD11C1 daily files (Wan, 2013; Wan et al., 2015). Here the Terra data set has been retrieved and the average monthly temperature over land has been derived by averaging the daytime and nighttime data sets.

The NCEP-NCAR and ERA5 reanalyses provide more detailed information for T at daily and monthly time scale, not only near the surface (2 m above ground) but also at several atmospheric levels, of which those of 1000, 925, 850, 700, 600, 500, 400 and 300 hPa are used in the study.

For the same levels, data for relative humidity, U, are also provided at the monthly scale; from the temperature and relative humidity, the dew point, T_d, can be estimated (equation (4) below). In addition, the ERA5 daily reanalysis provides independently the daily dew point for the surface level.

2.3   Atmospheric water data

As already mentioned, the relative humidity, U, is available at the monthly scale at several atmospheric levels for both reanalyses. In addition, the specific humidity, q (see equation (5) below), is independently available and was retrieved at the

levels of 850 hPa, and 300 hPa. The reanalyses fields also include data for the water vapour amount, W (also known as *vertically integrated water vapour*, or *precipitable water*[*] and expressed in mm or equivalently kg/m^2).

In addition, W is provided from satellite observations in two data sets, NVAP and MODIS. The NVAP data set is a model-independent dataset relying mainly on satellite measurements, from the NASA Pathfinder project (Vonder Haar et al., 2012). The monthly data for the period 1988-2009 over the globe are available in the form of a graph, which has been digitized here. For the more recent years, W is also available from the MODIS satellites Terra and Aqua mentioned above (Platnick et al., 2015; Hubanks et al., 2015). In addition, the MODIS platforms provide data for the column amount of ice (W_{CI}) and liquid water (W_{CL}) in the clouds, also known as *cloud ice water path* and *cloud liquid water path*, respectively; these are also used in the study.

2.4 Precipitation data

Gridded ground data for precipitation rate, P (mm/d), over land are available by the Climate Prediction Center's (CPC) unified gauge-based analysis of global daily precipitation for the period 1979 to present. This is based on gauge reports from over 30 000 stations, collected from multiple sources including national and international agencies. Quality control is being performed through comparisons with historical records and independent information from measurements at nearby stations, concurrent radar and satellite observations, as well as numerical model forecasts. Quality controlled station reports are then interpolated to create analysed fields of daily precipitation with consideration of orographic effects (Xie et al. 2007). The daily analysis is constructed on a 0.125° grid over the entire global land areas, and released on a 0.5° grid (Xie, 2010). This dataset has two components, the *retrospective version* which uses 30 000 stations and spans 1979-2005 and the *real-time version* which uses 17 000 stations and spans 2006-present; the latter have been planned to be reprocessed for consistency with the retrospective analysis. Here all data are used for both the daily and monthly scale.

Another gridded precipitation data set, this time extending also over the sea, is the data set of the Global Precipitation Climatology Project (GPCP), which combines gauge and satellite precipitation data over a global grid. The general approach is to combine the precipitation information available from each of several satellites and in situ sources into a final merged product, taking advantage of the strengths of each data type. Passive Microwave estimates are based on Special Sensor Microwave Imager/Special Sensor Microwave Imager Sounder (SSMI/SSMIS) data; infrared precipitation estimates are included using Geostationary Operational Environmental Satellite (GOES) data and Polar-orbiting Operational Environmental Satellite (POES) data, as well as other low earth orbit data and in situ observations (Adler et al., 2016). Monthly data are provided on a 2.5° grid and are available for the period 1979 to present. The GPCP daily analysis is a companion to the monthly analysis, and provides globally complete precipitation estimates at a spatial resolution of 1° and daily time scale from October

---

[*] The adjective *precipitable* for the water vapour amount is a misnomer: if the total water vapour amount in the atmosphere was indeed to precipitate in its entirety, this would violate the laws of thermodynamics.

150   1996 to the present. Although derived using both some of the same, but also some different, data sets and methods, compared to those used in the GPCP monthly analysis, the daily data add up to the monthly (Huffman, 2001; Adler, et al., 2017).

      The NCEP-NCAR and ERA5 reanalyses also provide gridded daily and monthly precipitation data.

      Information about snow is provided by satellite data. The most complete data set of this type is the snow cover extent for the Northern Hemisphere (NH), monitored via satellites by the US National Oceanic and Atmospheric Administration

155   (NOAA) from 1966 to present, updated monthly. Data prior to June 1999 are based on satellite-derived maps of NH snow cover extent produced weekly by trained NOAA meteorologists; after that date, they have been produced by daily output from the Interactive Multisensor Snow and Ice Mapping System. The data are provided on a Cartesian grid with 88×88 cells laid over a NH polar stereographic projection, where each grid cell has a binary value, indicating snow covered or snow free (see details in Robinson et al., 2012, and Estilow et al., 2015). Snow cover extent in the Southern Hemisphere is not currently

160   monitored.

2.5   Evaporation data

At present, the evaporation rate, E (mm/d), cannot be measured at large scales and is estimated only by models. Here the monthly data sets by the NCEP-NCAR and ERA5 reanalyses are used.

2.6   Data access and processing systems

165   There are lots of software applications to analyse and process gridded data. Here we are using free web platforms that are easy to use and allow direct reproducibility of the results by the interested reader; the links to these platforms are given in Table 1.

      Most of the processing in this study has been made via the Climate Explorer (climexp) system of the Royal Netherlands Meteorological Institute (Koninklijk Nederlands Meteorologisch Instituut; KNMI). This very powerful system combines access to many sources of data, including most of the data sets used here but also data from individual stations, and multiple

170   processing options. The data access includes, among other options, daily fields of observations and reanalyses, monthly observations and monthly reanalysis fields. The processing options include averaging over geographical areas (including over pre-specified or user defined "masks", i.e. polygons defined by a set of connected (x, y) points), aggregating at larger scales, computing zonal means, making time series and calculating their statistics, and plotting the fields.

      NASA's *Giovanni* online web environment is another useful tool for access, display and analysis of NASA's

175   geophysical data (Acker and Leptoukh, 2007). A similar system for NOAA's data, which also incorporates data for fields of additional sources, is the Web-based Reanalyses Intercomparison Tools (WRIT; Earth System Research Laboratory's Physical Sciences Division; see Smith et al., 2014).

      Access to some of the data which are not contained in the above three systems is provided by other platforms as specified in Table 1.

3 Atmospheric water

3.1 Atmospheric temperature and dew point

For the study of atmospheric water, air temperature is an important variable and thus we start with this. Figure 1 (left) shows the evolution of global average temperature at the level of 2 m above ground at the monthly and annual scale, according to both reanalyses data, NCEP-NCAR and ERA5. In addition, Figure 1 (right) depicts satellite data in comparison to reanalysis ones, but at a higher altitude. Specifically, the UAH satellite time series is used, which refers to the lower troposphere. Comparing this to reanalysis data at several pressure levels, we found that it roughly corresponds to weighted averages of those at the levels of 500 and 700 hPa with weights 0.62 and 0.38, respectively. Figure 1 shows a good agreement of all three information sources at both pressure levels. At the same time, they show a gradual increase of temperature, with about the same rate of increase. All three sources provide complete information for the last 40 years, while one of them, NCEP-NCAR, has a longer span, 68 years.

If we split the common 40-year period into two parts, we may compare the climatic values on a 20-year climatic scale and calculate the temperature increase. This is done in Table 2, where an increase of 0.38 °C can be seen for the globally averaged temperature using the ERA5 reanalysis, corresponding to 0.19 °C per decade. By reducing the time window of the period defining climate from 20 to 10 years, we can determine the difference of (a 10-year average) climate over 30 years, which is 0.56 °C, again 0.19 °C per decade. For the UAH satellite data set, which is less affected by urbanization because of the higher elevation, the 30-year difference is lower, 0.39 °C, or 0.13 °C per decade.

In addition, Table 2 provides similar information for the land and sea parts of the earth, in terms of average temperatures as well as dew points. The dew point, defined as the temperature at which the air must be cooled to become saturated with water vapour, is a more useful variable than temperature for the study of atmospheric water. The time evolution of both variables on earth, land and sea can be seen in Figure 2. All these are based on ERA5 reanalysis information, as this is the only one readily provided for further processing through the climexp platform, both for temperature and dew point at the surface level. As a means of verification, the MODIS surface temperature over land is also plotted in Figure 2, which compares well (albeit with a little bias) with the ERA5 temperature over land. It can be seen in Figure 2 and Table 2 that the evolution of the dew point is also increasing in the recent period, but the increase is lower than that of temperature.

A practical way to express what the increasing rates represent can be obtained by calculating an offset distance on earth, which moving poleward in the temperate zone, would offset the average decadal increase of temperature or dew point. This is given in the last column of Table 2 and is 31 km per decade for the surface global temperature and 21 km per decade for the lower troposphere temperature and the surface dew point. This conversion was based on the zonal temperature and dew point profiles shown in Figure 2 (upper right); for the temperate zone (±23.5° to ±66.5°) the fitted slopes in the profiles are ±0.68 °C/° and ±0.56 °C/°, respectively, while one degree of latitude corresponds to 111 km. Another way to express the same is through the height, which moving up would offset the decadal increase of temperature, using the lapse rate of the standard

atmosphere, 6.5 °C/km. As seen in Table 2, to offset the increase in the global earth temperature, one needs to climb uphill at a rate of 29 m per decade.

It is quite interesting to assess the zonal variation of the increase of temperature and dew point. This information is provided by Figure 3 where we plot the difference of the earth temperature and dew point (according to the ERA5 reanalysis) from their averages in the period 1980-99. A positive difference corresponds to an increase after 1999. It is important to note that the greater increases are located in the northern polar area. In the tropical zone, which is hydrologically most important as the main source of evaporated water, the increase is half the global average, while there is no increase at all in the dew point. The latter point is of highest hydrological significance.

3.2 Humidity

The transition from a temperature-based description of atmospheric processes to a more hydrologically meaningful one is provided by the Clausius-Clapeyron equation, i.e. the law determining the equilibrium of liquid and gaseous phase of water, which maps temperatures to saturation vapour pressures. Koutsoyiannis (2014b) has highlighted the probabilistic nature of the law by deriving it purely by maximizing probabilistic entropy, i.e. uncertainty. In particular, the law was derived by studying a single molecule and maximizing the combined uncertainty of its state related to:

(a) its phase (whether gaseous, denoted as A, or liquid, denoted as B);

(b) its position in space; and

(c) its kinetic state, i.e., its velocity and other coordinates corresponding to its degrees of freedom and making up its thermal energy.

Denoting the saturation vapour pressure as e and using the notion of the so-called natural temperature θ, with units of energy (joules) rather than temperature (kelvins), in accordance to the probabilistic principle that entropy is a dimensionless quantity φ, (specifically, $1/\theta := \partial\varphi/\partial\varepsilon_I$ with ε_I denoting thermal energy), the resulting equation is:

$$e = e_0 \exp\left(\frac{\xi}{\theta_0}\left(1 - \frac{\theta_0}{\theta}\right)\right) \left(\frac{\theta_0}{\theta}\right)^{\beta_B/2 - \beta_A/2 - 1} \tag{1}$$

where (θ_0, e_0) are the coordinates of the triple point of water (specifically, $\theta_0 = 37.714$ yJ corresponding to $T_0 = 273.16$ K, $e_0 = 6.11657$ hPa), ξ is the phase change energy (the amount of energy needed to break the liquid-phase bonds with other molecules), and β_A and β_B are the degrees of freedom of a water molecule in gaseous and liquid phase, respectively (specifically $\beta_A = 6$, $\beta_B \approx 18$). The same law can be written in more customary notation, in terms of absolute temperature in kelvins and using macroscopic quantities, as (Koutsoyiannis, 2012):

$$e = e_0 \exp\left(\frac{\alpha}{RT_0}\left(1 - \frac{T_0}{T}\right)\right) \left(\frac{T_0}{T}\right)^{(c_L - c_p)/R} \tag{2}$$

where (T_0, e_0) are again the coordinates of the triple point of water, R is the specific gas constant of water vapour ($R = 461.5$ J kg^{-1} K^{-1}, $\alpha := \xi R/k = \xi N_a$ (with k the Boltzmann's constant and N_a the Avogadro constant), c_p is the specific heat at constant pressure of the vapour and c_L is the specific heat of the liquid water. By substitution of the various constants we end up with the following form of the equation (Koutsoyiannis, 2012):

$$e := e(T) = e_0 \exp\left(24.921\left(1 - \frac{T_0}{T}\right)\right)\left(\frac{T_0}{T}\right)^{5.06} \tag{3}$$

This form is both convenient and accurate (more accurate than other customary forms, theoretical or empirical, as illustrated in Koutsoyiannis, 2012).

A state in which the vapour pressure e is lower than the saturation pressure $e(T)$ is characterized by the relative humidity:

$$U := \frac{e}{e(T)} = \frac{e(T_d)}{e(T)} \tag{4}$$

which serves as a formal definition of both the relative humidity U and the dew point T_d. Figure 4 depicts the evolution of the saturation water pressures $e(T)$ and $e(T_d)$ for the average temperature T and dew point T_d, as the latter are shown in Figure 2, while Table 3 shows their changes per 20-year climatic periods.

It is important to note that all above quantities and derivations do not depend on the presence or not of other atmospheric gases and hence on the air pressure p. To take account for the other gasses in the air, which constitute the biggest part, known as the *dry air*, we use the specific humidity:

$$q := \frac{M_v}{M_v + M_d} = \frac{\rho_v}{\rho_v + \rho_d} \tag{5}$$

where M_v and M_d are the masses of vapour and dry air in a certain volume V, and ρ_v and ρ_d the corresponding densities. The evolution of specific humidity at two atmospheric levels, 850 and 300 hPa, according to the NCEP-NCAR and ERA5 reanalyses, is depicted in Figure 5 for the entire earth as well as the land and sea parts. For the 850 hPa level the two sources of data agree to each other: they indicate fluctuation over time, with no monotonic trend. The climatic differences according to the NCEP-NCAR reanalysis are shown in Table 4 where it is remarkable that in the land part at the 850 hPa level the difference is negative. For the 300 hPa level the two sources of data diverge substantially and, most importantly, the NCEP-NCAR suggests a decreasing trend while ERA5 suggests an increasing trend. We will examine this divergence in section 3.3. Table 4 shows that the change in the NCEP-NCAR data is negative not only in land, but also in the sea part and the entire earth.

To connect specific humidity to pressures, we use the law of ideal gases, which again can be derived by maximizing probabilistic entropy (Koutsoyiannis, 2014b) and takes the form:

$$pV = N\theta \tag{6}$$

where p is the pressure and N the number of molecules. Writing this law separately for water vapour and dry air ($e\,V = N_w\,\theta$, $(p - e)\,V = (N - N_w)\,\theta$, where N is the total number of molecules in volume V, of which N_w are water molecules) after algebraic manipulations we find:

$$q = \frac{\varepsilon e}{p - (1 - \varepsilon)e} \tag{7}$$

265   where ε is the ratio of the molecular mass of water to that of the mixture of gases in the dry air, i.e., $\varepsilon = 18.016/28.966 = 0.622$.

It has been a common assumption, based on the Clausius–Clapeyron relationship, that the global atmospheric water vapour should increase by about 6%–7% per °C of warming (e.g. Wuebbles et al., 2017). In turn, this assumption is based on the conjecture that on the planetary scale, relative humidity will remain roughly constant, and hence specific humidity is projected to increase in a warming climate (IPCC, 2013, p. 91; see more quotations from the IPCC report in Koutsoyiannis,
270   2020b). Indeed, combining equations (3), (4) and (7), and considering that $e \ll p$ we find:

$$q \approx \frac{\varepsilon U e_0}{p} \exp\left(24.921\left(1 - \frac{T_0}{T}\right)\right)\left(\frac{T_0}{T}\right)^{5.06} \tag{8}$$

It is then easy to verify that for a certain atmospheric level (p = constant) the following relationship holds true:

$$\frac{\mathrm{d}q}{q} \approx \frac{\mathrm{d}e}{e} = \left(24.921\frac{T_0}{T} - 5.06\right)\frac{\mathrm{d}T}{T} + \frac{\mathrm{d}U}{U} \tag{9}$$

Under the assumption that U is constant ($\mathrm{d}U = 0$), irrespective of the increase of temperature, it is seen that for $T = T_0 = 273.16$ K, $\mathrm{d}q/q = 7.3\%$ $\mathrm{d}T$, while for $T = 25\,°C = 298.15$ K, $\mathrm{d}q/q = 6\%$ $\mathrm{d}T$, in agreement with IPCC.

However, despite the conjecture $\mathrm{d}U = 0$ being widely accepted, the real-world data do not confirm it. As we have
275   already seen in Figure 3, in the tropical area, which is most significant as a source of atmospheric moisture, the dew point (and hence e) remains virtually constant, despite the fact that the temperature (and hence $e(T)$) increases. Clearly, this means that the relative humidity U has decreased with the increase of temperature. This appears to be the case in all of the time series we examined (entries 6 and 7 in Table 1). This result is in agreement with an earlier study by Wang et al. (2008) who concluded that atmospheric temperature and water vapour trends do not follow the conjecture of constant relative humidity over North
280   America.

By combining the time series of relative humidity with those of temperature (entries 3 and 4 in Table 1) and using equations (3) and (4), we constructed in Figure 6 the vertical profile of the difference of average water vapour pressure $e(T)$ and $e(T_d) = U\,e(T)$ over land at levels of atmospheric pressure ranging from 1000 to 300 hPa. The focus on the land part of the earth is justified because most of hydrological processes are occurring in this part. For the NCEP-NCAR data, the differences
285   plotted in the figure are of the 30-year climatic periods 1948-77 and 1990-2019 and for the ERA5 data of the 20-year climatic periods 1980-99 and 2000-19. If the assumption of unchanging relative humidity was valid ($\mathrm{d}U = 0$) then the profile of the actual vapour pressure $\Delta e(T_d)$ would be proportional to the saturation water pressure $\Delta e(T)$, i.e. $\Delta e(T_d) = U\,\Delta e(T)$. The resulting

curves would then be the dotted lines in Figure 6 corresponding to the actual $\Delta e(T)$ of the two periods but with relative humidity, U, estimated from the first climatic period (as it was assumed $dU = 0$). However, the real $\Delta e(T_d)$ series depart dramatically from these dotted lines. It is notable that for the NCEP-NCAR data it even becomes negative for a large part of the troposphere ($p < 700$ hPa or elevation > 3 km).

We may try to roughly approximate equation (9) by:

$$\frac{dq}{q} \approx \frac{de}{e} \approx C\left(24.921\frac{T_0}{T} - 5.06\right)\frac{dT}{T} \tag{10}$$

with a constant parameter C, which would be unity if $dU = 0$ held true, but in fact it is much lower. Using weighted least squares on the data of Figure 6 we estimated $C \approx 1/3$. This suggests that, contrary to the IPCC (2013) expectation, the global atmospheric water vapour over land is increasing by only about 2% per °C of global warming. In this case we may expect a 4% increase of atmospheric water in the celebrated (yet contradictory) target of 2 °C of global warming. From a hydrological point of view, given the high variability and uncertainty of the processes (cf. the motto in the beginning of the article), a 4% change may be deemed negligible. Nonetheless, the analyses that follow indicate that even the reduced rate of 2% per °C of global warming may be overestimated, particularly if it be translated into intensification of hydrological cycle.

3.3   Water vapour and cloud water amounts

By integrating the specific humidity over a vertical column of air from a low altitude z_0 (typically the surface altitude) corresponding to air pressure p_0, to a high altitude z_1 (typically the tropopause) corresponding to air pressure p_1, we define the (vertically integrated) *water vapour amount*. Specifically, the water vapour amount is:

$$W := \frac{1}{\rho_w}\int_{z_0}^{z_1}\rho_v dz = \frac{1}{\rho_w g}\int_{p_1}^{p_0} q\,dp \tag{11}$$

where ρ_w (= 1000 kg/m³) is the liquid water density and g (= 9.81 m/s) is the gravity acceleration.

The study of the temporal variation of W is much more informative than q or e because of the vertical integration of information. Both NCEP-NCAR and ERA5 reanalyses provide data for this variable (entries 12 and 13 in Table 1). In addition, we have satellite observations of W (entries 10 and 11 in Table 1), one of which (MODIS) gives also layered information. Figure 7 depicts the evolution of W according to all sources of information, for the entire earth as well as the land and sea parts. The NCEP-NCAR and ERA5 reanalyses agree impressively well to each other: they indicate fluctuation over time, with no monotonic trend. The NVAP satellite data also agree on the average, indicating no trend. However, the most recent MODIS satellite data suggest a decreasing trend, just the opposite of the IPCC expectations discussed above. As seen in Figure 8, which provides layered information for the MODIS data, the decreasing trend is more pronounced in the upper atmospheric levels (440 to 10 hPa). This observation, compared to Figure 5 (right) and in view of the above discussion (related to Figure 5 and Table 4) about the divergence of specific humidity trends at 300 hPa between the NCEP-NCAR and ERA5 reanalyses, confirms

315 the former and falsifies the latter. The climatic differences in *W* according to the NCEP-NCAR reanalysis, which covers a longer (68-year) period, are given in Table 5, where it can be seen that there is a decrease not only in the land part, but also in the entire earth.

For completeness, of the discussion about atmospheric water, Figure 9 depicts the variation of the cloud water amount in ice and liquid phase according to MODIS satellite data. Again, no monotonic trend is seen. Compared to the water vapour

320 amount (Figure 8), the cloud water is a very small quantity (two orders of magnitude smaller).

4 Precipitation and evaporation

While the analysis of atmospheric water in the previous section signifies *potentialities* at the hydrological cycle intensity, the analysis of precipitation rate signifies *actualities*. While, as already mentioned, the potentiality (the global atmospheric water vapour) was expected by IPCC to increase by about 6%–7% per °C of warming, the actuality (the precipitation rate) should be

325 lower. Specifically, according to IPCC's latest (Fifth) Assessment Report (IPCC, 2013, p. 91):

It is virtually certain that, in the long term, global precipitation will increase with increased GMST. Global mean precipitation will increase at a rate per °C smaller than that of atmospheric water vapour. It will likely increase by 1 to 3% °C⁻¹ for scenarios other than RCP2.6. For RCP2.6 the range of sensitivities in the CMIP5 models is 0.5 to 4% °C⁻¹ at the end of the 21st century. […] *Changes in average precipitation in a warmer world will exhibit substantial spatial*

330 *variation under RCP8.5.*

The rate of increase of precipitation, necessarily accompanied by an equal rate of increase of evaporation, has been known as sensitivity of the hydrologic cycle (or hydrological sensitivity). The smaller rate, compared to that in atmospheric water, has been estimated based on climate model simulations. Furthermore, Kleidon and Renner (2013; see also Kleidon et al., 2015), based on analytical calculations and thermodynamics, have estimated a hydrological sensitivity of 2.2% C⁻¹, within the

335 IPCC "very likely" range. Even accepting this IPCC assertion, it may be puzzling why hydrologists have given so much energy in studying hydrological impacts that are a priori framed in the range of 1% to 3% per °C. For in hydrology such percentages are negligible compared to the natural variability and the uncertainty even in the measurement of precipitation. Moreover, since the potentiality part (the expected increase of atmospheric water) has been already questioned, we may expect that in the actuality context the changes in precipitation are even less recognizable than implied by IPCC.

340 Indeed, Figure 10, which depicts the evolution of precipitation rate on earth and its land and sea parts, based on gauged, satellite and reanalysis information, suggests that precipitation fluctuates through the seasons and also through the years, but without a monotonic trend. The marked differences among the various sources of information are also indicative of substantial uncertainty in the estimation of precipitation.

The snow part of precipitation is also interesting to examine, as snow is more directly related to temperature. Figure 11

345 depicts the evolution of the snow cover in the Northern Hemisphere. Despite temperature increase, no noticeable change

appears on the annual basis. However, there are perceptible changes in the seasonal variation: in the most recent period the snow cover has decreased during the summer months and increased during the autumn and winter months.

As already mentioned, the evaporation rate is difficult to estimate and even more so to measure. The available gridded data come from reanalyses. Their plots in Figure 10 again show fluctuations through the seasons and through the years, and no monotonic trends.

Overall, the preceding data and analyses, particularly those of atmospheric water, can hardly support the intensification of the global hydrological cycle. Certainly, they reveal changes but the changes appear as multiyear fluctuations, not as consistent trends. These fluctuations do not correspond to popular hypotheses attributing changes to global warming. The above results are not exceptionally new. Indeed, Sun et al. (2012) reported a near-zero temporal trend in global mean precipitation for the period 1940–2009. Nonetheless, our results are dissimilar (or opposite) to the vast majority of studies reporting intensification. The reasons of dissimilarities are explained in Appendix A. Additional analyses, which show absence of intensification and, more recently, deintensification, in terms of precipitation extremes, are given in Appendix B.

The reasons for the failure of the popular hypothesis of intensification include these two: (a) the unsupported (and eventually falsified) conjecture that the relative humidity should be constant and (b) the oversimplification of the representation of natural process, which neglects or underrates important mechanisms that affect the atmospheric water more than those related to the greenhouse effect. Among these, mostly unpredictable or unaccounted for, mechanisms are: (a) the tropospheric aerosols (Wu et al., 2013) affecting radiation while enabling condensation of water vapour and formation of cloud droplets, (b) the vapour buoyancy feedback which stabilizes tropical climate by increasing the outgoing longwave radiation (Seidel and Yang (2020)[*], (c) the complex role of land use changes on climate (Pielke et al,, 2016), and (d) the coupled atmospheric-ocean circulation fluctuations, such us the El Niño Southern Oscillation (ENSO; e.g. Trenberth et al., 2005, who concluded that the precipitable water variability for 1988–2001 is dominated by the evolution of ENSO and especially the structures that occurred during and following the 1997–98 El Niño event).

5   Water balance

5.1   General framework and assumptions

The analyses of atmospheric water, as well as those of precipitation and evaporation, reveal two important points: (a) all processes fluctuate in time at all time scales and (b) no monotonic trends that would be attributed to temperature increase appear in any type of data. In some cases (e.g. satellite observations of water vapour amount) there appear some trends, which, however, are opposite to established expectations. Here we treat them as irregular fluctuations, which appear as monotonic trends because of the limited time window of observation. Consequently, in subsequent analyses we make all estimations on

---

[*] Perhaps this may explain the zonal distribution of the difference of the earth temperature and dew point shown in Figure 3, but this needs a great deal of additional work to investigate.

375   the basis of stationarity. It must be stressed that stationarity does not mean absence of change. It simply means that the change, however large, resists a deterministic description and hence a stochastic description becomes more appropriate and powerful (Montanari and Koutsoyiannis, 2014; Koutsoyiannis and Montanari, 2015). Additional information of this choice is provided sections 6.2 and 6.3.

A rather impressive result, shown in Figure 10 (upper) is that the precipitation and evaporation over the entire earth in
380   the NCEP-NCAR reanalysis agree very well to each other, indicating conservation of mass, a property that is not granted in reanalyses. Indeed, on annual time scale, the differences between the global precipitation and evaporation are small, ranging between +0.5% and –4.1%. This provides a good basis for estimating the water balance in terms of fluxes in the hydrological cycle. The ERA5 reanalysis is not as good in this respect as the NCEP-NCAR one. We note, though, that even the small differences on the global scale are amplified when we examine the land and sea separately. This is seen in Figure 12, which
385   depicts the water balance derived from the difference of precipitation and evaporation at land and sea. Here the fluxes were converted from mm/d used in other analyses to km^3/year, considering that the earth has an area of 510 072 000 km^2, of which 28.44% is land and 71.56% sea. The amplification of discrepancies (a known effect when taking differences of two processes) is evident in Figure 12. In particular, the figure shows that the ERA5 reanalysis is, in a systematic manner, far from conserving water mass in the period prior to 2000, but it was much improved in the years 2000-15, worsening again in the most recent
390   years. The NCEP-NCAR does not indicate systematic error patterns.

Before proceeding to water balance estimation, we stress the importance of that balance in quantifying the availability of water resources. Contrary to most other common goods (e.g. fossil fuels and metals) that are subject to depletion, water resources are renewable, not reserves. In this respect, hydrology should fight the common misrepresentation (or even misconception in reports from media and information provided to the wider public and decision makers), implied by the
395   popular use of graphs like that in Figure 13. It is not the purpose of this study to examine or question the correctness of the information on the graph, which shows where on earth water is stored. However, the graph gives wrong impressions or messages. As an example, it suggests that the vast majority of liquid freshwater on earth is groundwater, while the river water is almost negligible. However, considering the renewable character of water resources, the truth is just the opposite: the vast majority is river water, while groundwater is almost negligible, as will be detailed below. For that reason, a caution stamp is
400   added to Figure 13.

We now proceed to calculations, noting that their precision will be of the order of 100 km^3/year; thus, any calculated quantity is rounded off to multiples of this value. The water balance at the land and sea parts of the earth is written, respectively:

$$\frac{\mathrm{d}\underline{S}_L}{\mathrm{d}t} = \underline{P}_L - \underline{E}_L - \underline{R} - \underline{G}, \qquad \frac{\mathrm{d}\underline{S}_S}{\mathrm{d}t} = \underline{P}_S - \underline{E}_S + \underline{R} + \underline{G} \tag{12}$$

where $\underline{P}_L$ and $\underline{P}_S$ are the precipitation flux over land and sea, respectively, $\underline{E}_L$ and $\underline{E}_S$ are the evaporation flux over land and sea, respectively, $\underline{R}$ and $\underline{G}$ are the surface runoff and submarine groundwater discharge to the sea, respectively, $\underline{S}_L$ and $\underline{S}_S$ are
405   the storages at land and sea, respectively, and t is time (see Figure 14). Underlined symbols denote stochastic variables or

stochastic processes. Assuming that the water density is 1000 kg/m^3 (i.e. neglecting variation due to temperature), the fluxes can be expressed as volumes per time, which in turn are rates multiplied by areas; for example, $\underline{P}_L := \underline{P}A_L$ is the precipitation flux over land [L^{3}T^{-1}], where $\underline{P}$ is the precipitation rate [LT^{-1}] averaged over land, and A_L [L^2] is the land area. Assuming zero storage change in the atmosphere (an assumption supported by the analyses of section 3), we can write:

$$\frac{d\underline{S}_L}{dt} + \frac{d\underline{S}_S}{dt} = 0 \tag{13}$$

410   Combining (12) and (13) we find:

$$\underline{P}_L + \underline{P}_S = \underline{E}_L + \underline{E}_S \tag{14}$$

Hence, we can write:

$$\underline{P}_L - \underline{E}_L = \underline{E}_S - \underline{P}_S =: \underline{A} \tag{15}$$

where $\underline{A}$ is the advection, i.e., the flux of water mass from sea to land through atmospheric processes.

5.2   Changes in storage

Changes in land and sea water storage are small but not negligible. With reference to Figure 13, the land storage can be
415   decomposed in five compartments, ice, $\underline{S}_I$, snow, $\underline{S}_S$, biosphere, $\underline{S}_B$, surface water, $\underline{S}_{SW}$, and groundwater (including soil water), $\underline{S}_{GW}$. Hence:

$$\frac{d\underline{S}_L}{dt} = \frac{d\underline{S}_I}{dt} + \frac{d\underline{S}_S}{dt} + \frac{d\underline{S}_B}{dt} + \frac{d\underline{S}_{SW}}{dt} + \frac{d\underline{S}_{GW}}{dt} \tag{16}$$

For the ice loss, Syed et al. (2009), on the basis of the average of two earlier studies, estimated a quantity of –284 ± 59 km^3/year[*], which refers to Greenland and Antarctica. A newer study by Velicogna and Wahr (2013), based on GRACE satellite data, found a change of –258 ± 41 km^3/year for Greenland and –83 ± 49 km^3/year (or somewhat larger using another model)
420   for Antarctica. As noted by Velicogna et al. (2014) the total mass loss is controlled by only a few subregions in Greenland and Antarctica and are mostly due to ice dynamics, where the latter term means the motion within large bodies of ice; in turn, this is controlled mainly by the temperature and strength of their bases, rather than the atmospheric temperature (see also Hanna et al. 2020). However, IMBIE (2020) suggested that in Greenland the shares of losses due to ice dynamics and surface processes are equal (about –75 km^3/year each one; their Table 1 for years 1996-2018). Furthermore, IMBIE (2018, Table 1) estimated
425   for the Antarctic Ice Sheet a loss of −109 ± 56 km^3/year for years 1992-2017, which becomes −219 ± 43 km^3/year for years 2012–2017 (without specifying the share of ice dynamics). The disagreements among different estimates are highlighted by the results of the study, based on satellite data, by Zwally et al. (2015), who reported that the mass gains of the Antarctic Ice

---

[*] Some of the reviewed studies provide estimates in terms of volume (km^3), while some other in terms of mass (Gt). Here we convert all quantities in the former form, assuming constant density, so that 1 Gt corresponds to 1 km^3 of water.

Sheet exceed losses by 82 ± 25 km^3/year (or somewhat greater, 112 ± 61 km^3/year, using a different data set); the study triggered controversy with several comments and replies. Disagreements are also exemplified in Hanna et al. (2020), who,

430   despite the new observational (especially satellite) data and the recent efforts, find that significant discrepancies remain with respect to absolute mass balance values for the East Antarctic Ice Sheet, while for the Greenland Ice Sheet absolute values vary by ~100-300 km^3/year between recent years. In a reconciled estimate for the entire area covered by glaciers, including regions distinct from the Greenland and Antarctic Ice Sheets, Gardner et al. (2013), using satellite gravimetry and altimetry, and local glaciological records, suggested a global budget of -259 ± 28 km^3/year for 2003–2009. In line with the latter study,

435   here we assume $E[d\underline{S}_I/dt] = -300$ km^3/year for the contemporary period.

For the snow storage, the snow data analysed in section 4 allow the assumption of a zero mean change at the annual and overyear scales, even though at seasonal scales it is certainly not negligible (see Figure 11). For the water in the biosphere, there must be a positive change as in the 21st century the earth has been greening, mostly due to CO_2 fertilization effects (Zhu et al., 2016) and human land-use management (Chen et al., 2019). Specifically, the MODIS data show a net increase in leaf

440   area of 2.3% per decade (Chen et al., 2019) but it is difficult to translate this into a net increase in water stored in the biosphere. Nonetheless, we do not expect this change to be large (in comparison to other changes) and we will neglect it.

Surface water storage has been affected by substantial depletion of several large natural water bodies in the past, mostly due to overexploitation of their water, while at the same time it was enhanced by the construction of artificial reservoirs. The Caspian Sea changes, often associated to the sea level changes, are large but alternating in sign (Chen et al., 2017) and thus

445   there is no reason to assume a balance value other than zero. The Aral Sea has dramatically shrunk in volume since 1950 (Gaybullaev et al., 2012; Cretaux et al., 2019) and has thus contributed in a negative water balance in land (and positive in sea, corresponding to sea level rise), but stabilization is a likely possibility for the present and future. Reservoir impoundment, has also affected the water balance after the construction of reservoirs (Chao et al., 2008). However, given that the number of new reservoirs has been diminished after 2000, while a reservoir has zero further effect on the long-term water balance after its first

450   fill, we do not expect further substantial effects[*]. For these reasons, we assume a zero (further) change of surface water storage for the contemporary period.

For the groundwater storage change, which we expect to be significant, Wada et al. (2010) have estimated a global depletion rate of 283 ± 40 km^3/year in 2000, which in Wada et al. (2016, their Fig. 1) becomes 292 km^3/year over the period 1900–1999, while Wada (2016, their Fig. 6a) give an estimate of about 200 km^3/year for the year 2000. In their recent review

455   article, Bierkens and Wada (2019) report estimates from several studies, based on global hydrological models and GRACE data, which vary from 90 to 510 km^3/year for the recent years. These justify an average estimate of $E[d\underline{S}_{GW}/dt] = -300$ km^3/year for the contemporary period.

---

[*] Chao et al. (2008) in their estimates include a seepage effect into the future, which they base on arbitrary assumptions, among which is the continuation of a seepage loss into the future at a rate inversely proportional to the square root of time. Noting that this assumption would lead to losses that diverge to infinity as time increases, while the water from the loss (as that of reservoir withdrawal) remains in the land water storage, here we disregard this assumption.

In summary, we have assumed:

$$\mathrm{E}\left[\frac{\mathrm{d}S_\mathrm{I}}{\mathrm{d}t}\right] = \mathrm{E}\left[\frac{\mathrm{d}S_\mathrm{GW}}{\mathrm{d}t}\right] = -300\,\mathrm{km}^3/\mathrm{year}\,, \qquad \mathrm{E}\left[\frac{\mathrm{d}S_\mathrm{SA}}{\mathrm{d}t}\right] = \mathrm{E}\left[\frac{\mathrm{d}S_\mathrm{B}}{\mathrm{d}t}\right] = \mathrm{E}\left[\frac{\mathrm{d}S_\mathrm{SW}}{\mathrm{d}t}\right] = 0 \qquad (17)$$

Accordingly, the water storage in land has a total loss of 600 km³/year, which is a gain to the storage in the sea. This
mass gain corresponds to an increase of sea level equal to 1.64 mm/year. Half of this (0.82 mm/year) corresponds to
groundwater depletion (i.e. conversion of groundwater to seawater, as water mass cannot disappear nor can it be stored in the
atmosphere, where it initially moves by evaporation in irrigated areas). This is clearly an anthropogenic effect in its entirety
and is likely to remain, if not increase, in the foreseeable future. It is also a clear mark of unstainable water management. An
equal portion of sea level rise (0.82 mm/year, according to this study) is due to ice loss from land, but as already mentioned,
most part of it is not attributed to anthropogenic causes. The latter value is consistent with the estimates by Marzeion et al.
(2015), which range between 0.70 to 0.96 mm/year for the period 2003-09. For comparison, an almost equal amount, 0.77
mm/year according to Llovel et al (2014), or higher, 1.31-1.32 mm/year, according to WCRP (2018) is due to thermal
expansion. One may hastily tend to attribute this latter amount to anthropogenic global warming, neglecting natural variability
(including the succession of El Niño/La Niña events). Such negligence may be problematic: for undoubtedly, neither the 125
to 140 m sea level rise in the last 20 thousand years (Fleming et al., 1998) nor the sea level change of a range of up to 600 m
in the last 500 million years (Hallam, 1984; van der Meer et al., 2017) are anthropogenic.

5.3   Submarine groundwater discharge

The submarine groundwater discharge (or groundwater outflow to the sea) is the most difficult to estimate. A most recent
estimation has been conducted by Zhou at al. (2019) using a water budget approach at high resolution. They examined the
near-global coastal recharge areas (60°N to 60°S) and provided spatially distributed high-resolution estimates using average
infiltrating runoff from three land surface models (MOSAIC, NOAH, and VIC) obtained from NASA's Global Land Data
Assimilation System. They concluded with a near-global estimate of submarine groundwater discharge at 489 ± 337 km³/year,
noting that 56% is the export in tropical coasts, while mid-latitude arid regions export only 10%. In line with this recent
estimate, here we assume:

$$\mathrm{E}\left[\underline{G}\right] = 500\ \mathrm{km}^3/\mathrm{year} \qquad (18)$$

This choice needs some further explanation, as it is substantially (by 4-5 times) lower than the commonly adopted
earlier estimates, such as those by Shiklomanov and Sokolov (1985), and Zekster and Loaiciga (1993, citing Zektser and
Dzhamalov, 1981), which are 2200 and 2400 km³/year in the two studies, respectively, or about 5-6% of total runoff; the latter
quantity had been estimated to 46 800 and 38 000 km³/year in the two studies, respectively.

An even earlier, yet frequently cited, estimate by Lvovitch (1970), is somewhat lower, 1600 km³/year. Lvovitch did not
obtain this estimate himself but cites Nace (1964) for suggesting it, also noting that he finds it reasonable. Surprisingly

however, in another article, Nace (1967) clearly states that this value is arbitrary. Specifically, his footnote to "*Ground-water outflow to oceans*" in his Table 1 (which, notably, mixes water stocks and fluxes) is verbatim: "*Arbitrarily set equal to about 5 percent of surface runoff*". In addition, it seems that Nace has made a numerical error as the value he gives for surface runoff is 38 000 km^3/year; hence, the 5% thereof is 1900 km^3/year rather than 1600 km^3/year.

490   These old guesses, rather than estimates, have been adopted (by citing the above studies) in most papers and textbooks until now, either in its percentage version (e.g. 5% in Dai and Trenberth, 2002, who cite Lvovitch, 1970) or in absolute values, mostly adopting Shiklomanov and Sokolov's (1985) values of 2200 and 46 800 km^3/year for the groundwater and total runoff, respectively (Dingman, 1994; Khedun and Singh, 2017).

Values even much higher than those have also been published; for example, in a celebrated paper, Oki and Kanae (2006)
495   assert:

some part of the water, approximately 10% of total river discharge [Church, 1996], *infiltrates to deep underground and will never appear as surface water but discharge into the ocean directly from groundwater.*

And, indeed, Church (1996) contains this 10% estimate, but also refers to a wide range, between 1% and 10%, without performing own analyses. He further implies that the 10% estimate was proposed by Zektzer et al. (1973). However, this value
500   in Zektzer et al. refers to the groundwater discharge to the Lake Ladoga and, coincidentally, to some results for the United States by Nace (1969). In general, the review and methodological paper by Zektzer et al. (1973) does not contain any information on the global scale.

The only case of a low estimate, of the order of that used here, is in Nace's (1970) paper, which appears to be the first in history quantitative analysis of the groundwater discharge to the sea. Surprisingly, only three years after his 5% "*arbitrarily*
505   *set*" guess, Nace (1970) came up with the quantitative estimate of 7 000 m^3/s, or about 220 km^3/year, that is 7-9 times smaller (depending on the correction or not of his aforementioned error) than his own initial guess. Subsequently he remarks:

The average total runout [i.e., submarine groundwater discharge] *then would be about 7 000 m^3 s^{-1}. This is less than 1 percent of estimated surface runoff. While the calculation is wholly hypothetical, it is based on liberal assumptions. In order to be significantly large the value would have to be greater by a factor of 5. Evidently, runout is negligible in*
510   *relation to the world water balance, though it is significant within some regions.*

It is thus likely that behind the initial 5% guess, as well as its eager adoption by later researchers, was a desire "*to be significantly large the value*". However, one may think that such an overestimation of the groundwater flux, in addition to overemphasizing the groundwater stock (which appears very large in Figure 13), may have offered bad service both to science and water management, as it may have encouraged the overexploitation (far beyond the natural recharge rate) of groundwater,
515   with consequences such as the subsalinization of coastal aquifers, the subsidence of land areas and the rise of sea level. The quotation and the whole story may also be didactic as it illustrates the adverse consequences of convictions about what "*the value would have to be*", else known as *confirmation biases.*

The fact is that the estimate of 220 km³/year has remained unnoticed in the literature. The general preference has been to quote, misquote, or confirm the 5% guess, as indicated in the above references. To complete this timeline of consistent distortion, the following excerpt from Zhou et al. (2019) is quite indicative:

Integrated over the near-global coastline, the total annual volume of fresh SGD [submarine groundwater discharge] *is 489 km³/year ±337 km³/year, or 1.3% of river discharge (Dai & Trenberth, 2002), in line with previous estimates (Church, 1996; Zekster & Loaiciga, 1993).*

While, as already stated, here we fully adopt the estimate of Zhou et al., which is closer to Nace's (1970) estimate than to any other, the authors' assertion that their value of 1.3% is in line with those they cite (which as explained above are 5% to 10%, or 4 to 8 times larger, even though Church mentions the 1% case) is surprising. Perhaps a statement such as the above, which hides big disagreements among estimates, hinders the discussion of an important issue. Without an extensive discussion the issue remains open; hopefully the discussion here has shed some light but it is not the scope of this article to resolve this open problem.

5.4   Final quantification of water balance

The above detailed review and discussion was about small quantities in water balance. Fortunately, the big quantities, precipitation and evaporation over land and sea, are estimated more accurately (on a percentage basis) and the NCEP-NCAR reanalysis provides a good basis for estimation. As already stated, the error in satisfying equation (14) is +0.5% and –4.1% on the annual scale. Given the above assumptions, the unknown quantities are the runoff R and the advection A. Their expectations will be:

$$E[\underline{R}] = E[\underline{P_L}] - E[\underline{E_L}] - E[\underline{G}] - E\left[\frac{dS_I}{dt}\right] - E\left[\frac{dS_{GW}}{dt}\right], \qquad E[\underline{A}] = E[\underline{E_L}] - E[\underline{P_L}] \tag{19}$$

while, with the numerical values assigned to the last three terms in the former equation, we will have $E[\underline{R}] - E[\underline{A}] = 100$ km³/year.

To proceed, we assume that the precipitation values are more reliable, as they are crosschecked with satellite data, and we adjust the evaporation data so as to precisely satisfy equation (14). A sensitivity analysis of the effect of allocating the error in the resulting water balance is shown in Table 6. If we allocate the entire error to sea evaporation, the resulting mean runoff is 30 800 km³/year while if we allocate it to land evaporation it increases to 37 300 km³/year. However, a proportional adjustment in both land and sea seems more reasonable. In this case the resulting average runoff is 32 000 km³/year and the advection 31 900 km³/year. All these quantities are graphically illustrated in Figure 14. The figure includes also information of the climatic variability on a 30-year climatic scale of the averages given; explanations about the values noted will be given in section 6.3. We stress that variability does not coincide with uncertainty. The former corresponds to the fact that climate is

varying. While climatic variability translates to uncertainty when future predictions are cast, there are additional sources of uncertainty, such as errors in the data and assumptions.

If we apply equations (19) dropping the expectations, i.e. using the time varying values, what we will get is not the actual runoff and advection, because some storage changes not included in the equation, such as in snow, in soil water and in
550 atmospheric water, are not identically zero; rather their mean is zero. On the annual basis it may be expected that the error is negligible but on monthly scale it will be present. Nonetheless, such an exercise is useful to conduct to see the temporal variability. This is depicted in Figure 15, where for rigour in terminology we have replaced the terms "runoff" and advection" with "water balance from land" and "water balance from sea", respectively. The right panel of Figure 15 depicts the mean monthly averages, which differ remarkably. The differences are related to the within-year storages not included in the equation
555 and look quite reasonable. As the northern hemisphere dominates in land processes, it is reasonable to expect that in the period December-May the storage is increasing, while during July-October it is decreasing.

Compared to the popular estimates by Shiklomanov and Sokolov (1985), and Zektser and Dzhamalov (1981), which as already noted are 46 800 and 38 000 km^3/year, respectively, our estimate of mean total (surface and groundwater) runoff of 32 500 km^3/year is markedly lower. However, it is (almost precisely) equal to the estimate by Syed et al. (2009; their Table
560 6), which is based on observed terrestrial water storage changes from GRACE and reanalysis data. The latter study (in its Table 5) quotes also older estimates, since 1975, which range from 22 000 to 40 000 km^3/year. A newer monography by Dai (2016) provides an estimate at about 36 500 km^3/year, very close to the estimate by Zektser and Dzhamalov (1981), as well as to the value 38 450 km^3/year estimated by Ghiggi et al. (2019), based on GRUN for the period 1902 – 2014; the latter authors also report results from earlier studies ranging from 30 000 to 66 000 km^3/year. On the other hand, the recent study by Schellekens
565 et al. (2017) suggests a value of about 46 300 km^3/year, very close to that by Shiklomanov and Sokolov (1985). According to Schellekens et al. (2017), the terrestrial precipitation is 119 700 km^3/year (against 123 300 of the present study) and the evaporation 74 5000 (against 91 400 of the present study); thus, it is the difference in evaporation that makes the latter study inconsistent with the present one.

Figure 16 provides a comparison of runoff time series (or balances in land and sea) from the present study with earlier
570 studies. The differences in estimates are apparent and translate in a huge uncertainty about the true value of runoff. Apparent is also a satisfactory agreement of the present study with that of Syed et al. (2009). Some of the studies provide ensemble values, but in Figure 16 only the ensemble means are plotted (the upper limits of ensembles would exceed the plotting area). In view of the high uncertainty, it seems not meaningful to search for trends in runoff. We may notice, though, that in the time series of the present study, there appear higher values in recent years. These values correspond to increased rainfall in NCEP-
575 NCAR reanalysis over land. This, however, is not confirmed by the gauge and satellite observations (Figure 10), which, as already discussed, indicate falling trends. Therefore, the changes will be interpreted as irregular fluctuations within a frame of very high uncertainty, rather than monotonic trends, which clearly are not.

The latter interpretation is consistent with the results of a large-scale study of trends in the flow of 916 world's largest rivers by Su et al. (2018). The results, and specifically those in their Table 1 that take into account the long-term persistence,

show some trends, either positive (3.7% of the rivers) or negative (8.2% of the rivers). While negative trends are more common than positive in number, they have slightly lower slopes, so that, overall, the positive slopes slightly surpass the negative ones (9.1 vs. –7.2 hm^3/year).

5.5   Energy involved in the hydrological cycle

According to Figure 14, the total evaporation on earth (precisely equal to the total precipitation according to equation (14)) is 522 700 km^3/year and corresponds to 5.227×10^{17} kg/year of water flux. For average temperature of earth equal to 14.46 °C (Table 2), the latent heat of evaporation (calculated from Koutsoyiannis, 2012, eqn. (40)) is 2.467×10^6 J/kg. Thus, the total energy involved in the hydrological cycle is 1.290×10^{24} J/year or 1290 ZJ/year. This corresponds to 4.086×10^{16} W, which if reduced to the earth's area (5.101×10^{14} m^2) results in an energy flux density of 80 W/m^2, precisely equal to the value given by Trenberth et al. (2009). This is about half the global solar energy absorbed by the earth (161 W/m^2 according to Trenberth et al., 2009).

Compared to the human energy production, which in the past decade was about 170 000 TWh/year or 0.612 ZJ/year (corresponding to year 2014; Mamassis et al., 2020), the total energy involved in the water cycle is 2100 times higher. Put it differently, the total human energy production in a year equals the energy consumed (or released) by the hydrological cycle in about four hours.

6   Dealing with the future of water resources

6.1   Deterministic approaches: Climate model predictions vs. data

While most of climate impact studies have been based on the assumption that climate models provide plausible predictions (usually termed *projections*) of future hydroclimate, there is a number of studies that claimed that this cannot be true as, when compared with real data of the recent past (after the predictions were cast) or even earlier data (already known at the time of casting the prediction), prove to be irrelevant with reality (Koutsoyiannis et al., 2008, 2011; Anagnostopoulos et al., 2010). This becomes even worse if we focus on extremes (Tsaknias et al., 2016). Tyralis and Koutsoyiannis (2017) developed a theoretically consistent (Bayesian) methodology to incorporate climate model information within a stochastic framework to improve predictions. However, because of the bad performance of climate models, application of this methodology leads to increased uncertainty or, in the best case, in results that are indifferent with respect to the case were the climate model information is not used at all. In summary, as implied by Kundzewicz and Stakhiv (2010), climate models may be less "ready for prime time" and more ready for "further research".

To test if this is also the case on a global setting, here we use climate model outputs for monthly precipitation simulations for scenario runs for the period 1860-2100, from the Coupled Model Intercomparison Project (CMIP5), a standard experimental protocol for studying the output of coupled atmosphere-ocean general circulation models (AOGCMs). CMIP5 includes the models for the IPCC Fifth Assessment Report (https://esgf-node.llnl.gov/projects/cmip5/). The scenario used is

the already mentioned "RCP8.5" (frequently referred to as "business as usual", even though there is a lot of controversy about this, e.g. Burgess et al., 2020). The model outputs have again been accessed through the climexp platform (option Monthly CMIP5 scenario runs).

Comparison of model outputs with reality, as the latter is quantified by the satellite (GCPC) observations, is provided in Figure 17. As expected by the assumptions and speculations mentioned in section 3, climate models predict increase of precipitation after 1990-2000. This hypothetical increase is visible in Figure 17. However, real-world data do not confirm the increase. Noticeable is also the large departure of reality and model outputs in terms of the average global precipitation. All these observations support the claim that climate models dissent from the hydrological reality and they further illustrate the fact that the real-world precipitation has not been intensified according to the IPCC expectations.

6.2   Statistical approaches: Trends

The statistical counterpart of the endeavour to predict the future, namely the fitting of "trends everywhere", based on real data, and projecting them to the future has been quite popular among hydrologists in the 21st century, as seen in a surge of related articles. Specifically, this has been quantified by a bibliometric investigation by Iliopoulou and Koutsoyiannis (2020) showing that in the last decade almost 90% of the scientific articles related to precipitation, hydrology and extremes contain the word "trends".

The comprehensive study by Iliopoulou and Koutsoyiannis (2020) assessed the "trends everywhere" approach using long precipitation series (> 150 years). The study compared four cases of projection to the future, namely (a) the mean estimated from the entire record, (b) a local time average estimated from the recent past, (c) a linear trend fitted to the entire record, and (d) a local linear trend estimated from the recent past. The mean of the process is a neutral predictor of the future (zero efficiency) but turns out to be better than predictions based on trends. In other words, the predictive skill of the trend models is poor, worse than using the mean, reflecting a poor representation of a complex reality. The model based on the local time average (case b) of previous years proves to be the best of the four. The reason is that in real-world processes there is temporal dependence or persistence (see below). Hence, a local temporal average (of values of the recent past) can be a better predictor than the global (or the true) mean.

6.3   Stochastic approaches: Hurst-Kolmogorov dynamics

The failure of climate models and trends to describe reality does not imply that in reality there is no change. On the contrary, all data sets examined suggest change, but the simplistic assumption that there is virtually a single cause (i.e. CO_2 concentration increase) that produces change does not work. Also, the other simplistic assumption that a trend seen in the past will continue in the future cannot work too, as it manifests misrepresentation of stochastic patterns as deterministic trends, while formally the stochastic patterns should be described in terms of time dependence. More generally, history shows that attempts to foretell the unknown future within a deterministic paradigm, resulted in spectacular failures. Therefore, in the real-world hydrological

practice there has been a legacy of using stochastics, which reflects a different paradigm in both understanding and modelling natural processes (Koutsoyiannis et al., 2009; O'Connell et al., 2016).

Assuming that a real-world process x_τ is modelled as a stochastic process $\underline{x}_\tau$, where τ denotes discrete time, we can
645 monitor the changes at multiple time scales κ through the time-averaged process:

$$\underline{x}_\tau^{(\kappa)} = \frac{1}{\kappa} \sum_{i=(\tau-1)\kappa+1}^{\kappa\tau} \underline{x}_i \tag{20}$$

For small κ (e.g. daily scale) we usually call $\underline{x}_\tau^{(\kappa)}$ *weather* and for large κ (e.g. corresponding to 10, 30 or more years) we call it *climate*. We may notice that there is no qualitative difference between weather and climate. Both are varying in time, and the variation is quantified by the variance $\gamma(\kappa)$, as a function of time scale κ, a function termed the *climacogram* (Koutsoyiannis, 2010). For sufficiently large κ (theoretically as $\kappa \to \infty$), we may approximate the climacogram as:

$$\gamma(\kappa) \propto \kappa^{2H-2} \tag{21}$$

650 where H is termed the *Hurst parameter*. The theoretical validity of such (power-type) behaviour of a process was implied by Kolmogorov (1940). The quantity $2H - 2$ is visualized as the slope of the double logarithmic plot of the climacogram for large time scales. In a random process, $H = 1/2$, while in most natural processes $1/2 \le H \le 1$, as first observed by Hurst (1951). This natural behaviour is known as (long-term) *persistence* or *Hurst-Komogorov* (HK) *dynamics*. A high value of H (approaching 1) indicates enhanced presence of patterns, enhanced change and enhanced uncertainty (e.g. in future predictions). Additional
655 information on the relationship of Hurst-Kolmogorov dynamics with change can be found in Koutsoyiannis (2013) while the applicability of the law (21) to time scales as long as several million years can be seen in Markonis and Koutsoyiannis (2013).

Now, Figure 18 shows the climacograms of the different types of processes examined in this study and the different sources of information. It is evident that all processes are consistent with the HK dynamics. Seasonality has also a significant effect in some (but not all) of the processes. In most of the processes H is very high, 0.9 or even higher. A notable exception
660 is GPCP precipitation time series with $H = 0.64$. However, the NCEP-NCAR precipitation suggests much higher variability at all time scales and H close to 0.90.

High H values imply high climatic variability: assuming that the discrete time scale κ represents years, and that the law (21) is a good approximation for the annual and multiyear scales (an assumption verified in Figure 18), we can conclude that the climatic variability at scale κ, expressed through the coefficient of variation, is:

$$\frac{\sqrt{\gamma(\kappa)}}{\mu} = \frac{\sqrt{\gamma(1)}}{\mu} \kappa^{H-1} \tag{22}$$

665 For $\kappa = 30$ and $H = 0.9$, this implies a 30-year climatic variation equal to 71% of the annual variation, while this would be 18% if the process were random (if H were 0.5). Additional information on the consequences of the HK behaviour in changing our perception and modelling of climate can be found in Koutsoyiannis and Montanari (2007) and Koutsoyiannis (2011).

7   Concluding remarks

Arguably, climate has been changing for the entire 4.5 billion-year earth's history; this has already been confirmed and roughly quantified for the last 0.5 – 0.75 billion years in aforementioned studies (Markonis and Koutsoyiannis, 2013; van der Meer et al., 2017). A changing climate can hardly be described by a mean value; variability is also needed to be specified. For this specification we certainly need a measure of variation, which could be one of the standard measures (variance, standard deviation, coefficient of variation). But we also need to define how this variability decreases as the time scale increases. A parsimonious way to do the latter task is through the Hurst parameter, which, based on the data sets used, turns out to be very high, implying that the difference between weather and climate is not as dramatic as in common perception. In this respect, even if the established climatic hypotheses of an intensifying hydrological cycle, with rates of the order of 1%, were validated, hydroclimatic concerns would not be justified. In older times such rates of change would not be discussed at all; for the logical framework about precision was already formed in ancient times (see the motto in the beginning of the article).

In fact, the established climatic hypotheses on hydrological cycle are not validated by the data analysed. Relative humidity is decreasing in the entire atmosphere, instead of being constant. Specific humidity is increasing at a rate of about 1/3 of that implied by established hypotheses, as results from comparing two recent periods of climatic time scale. Integrated over the entire troposphere and viewed in continuous time, the water vapour amount is fluctuating without a monotonic trend, while there are differences even in the sign of local trends for different data sets. Precipitation and evaporation again fluctuate. The precipitation extremes and their frequencies also fluctuate (Appendix B). Fluctuations are successions of intensification and deintensification, with deintensification prevailing in the 21st century.

The water balance on land and sea appears to be lower than the standard figures of literature. The total evaporation on earth, precisely equal to the total precipitation, is estimated at 522 700 km^3/year and corresponds to a total energy flux of 1290 ZJ/year or 80 W/m^2. The surface runoff is estimated to be 32 000 km^3/year, while the submarine groundwater discharge appears to be only 1.5% of runoff or 500 km^3/year. The variability on climatic time scales of all water balance components is very large, in accordance to Hurst-Kolmogorov stochastic dynamics. The uncertainty in figuring out the global water balance is still high, despite the recent big data amounts. The sources of uncertainty are many and, as analysed in the study, need substantial additional efforts to quantify.

The most obvious anthropogenic signal in the hydrological cycle is the overexploitation of groundwater, which has a visible effect on sea level rise. Melting of glaciers has an equal effect, but in this case it is not known what part is anthropogenic as studies for polar regions attribute mass loss mostly to ice dynamics.

The above observations strengthen an earlier (Koutsoyiannis et al., 2009) envisagement of hydrological community's role. Instead of a passive role in assessing hypothetical hydrological impacts based on doubtful climate model outputs, an active role consistent with its history is possible. Indeed, hydrology has much more to offer to societies than prophesies of future catastrophes (cf. Koutsoyiannis, 2020a). During the 20th century, and particularly after the Second World War, hydrology, by supporting hydrotechnology, water management, and risk assessment and reduction, within a strong

international collaboration and a strong economy, has substantially contributed to life as a value, as well as to the quality and length of life (Appendix B, Figure B5).

Appendix A: Differences in the approach of testing

We clarify that here, to detect possible intensification on hydrological cycle, we use past information on the global scale. This is similar to the common practice of detecting global warming, where the temporal evolution of an observed, globally averaged, temperature is typically used. While the globally averaged temperature is a statistical quantity with doubtful physical meaning, the globally (or regionally) averaged precipitation and evaporation are physically meaningful as they represent fluxes of water mass or volume. Therefore, it may be puzzling why the same method as in temperature has not been applied to precipitation, yet intensification claims have been the norm. This methodology of testing alleged intensification of the hydrological cycle distinguishes this study from the plethora of other studies claiming intensification. More specifically, the differences of the current study with other studies include the following points.

- We do not refer to model projections for the future which predict intensification (like e.g. Ziegler et al., 2003; Madakumbura et al., 2019). And indeed, as evident in Figure 17, if we used the climate model simulations and not the actual data, we would "detect" intensification even for the past years, let alone the future in which the model-projected increase in rainfall is higher. There is plenty of reasons why one should avoid that, reasons referring both to the past and the future. In general epistemological terms, according to Bridgman (1966), when a statement purports to be about the future, it is a 'pseudo-statement'. In more specific terms, it has been shown that the skill of climate models for representing hydrological processes (in particular, precipitation), measured by studying the past performance, is practically zero (Koutsoyiannis, 2008, 2011; Anagnostopoulos et al., 2010; Tsaknias et al., 2016). This situation is epitomized in the title of the article by Stephens et al. (2010), as a "dreary state of precipitation in global models".

- We investigate the entire period that each data set allows, in order to see the patterns of changes, i.e. whether there are monotonic trends or fluctuations. If one focuses on a short period (like in the study of Wild et al., 2008, which is for 15 years), it is likely to obtain a monotonic trend (even though in Fig. 1 of Wild et al., 2008, consistent increasing appears for 8 years, not for the entire 15-year period they examine).

- We do not refer to specific regions like Canada (Déry et al., 2009; Creed et al., 2015), Amazon (Gloor et al., 2013), etc. Certainly, there are regions where precipitation is currently intensifying, while in earlier periods in those regions, or in other regions at the same period, are deintensifying. Even the cited studies speak about "trend reversals" in time or give alternating trend signs in different locations. Such temporal and spatial fluctuations, rather than monotonic trends, are the normal behaviour in natural processes (see section 6.3). Furthermore, we do not focus on specific seasons of the year. There is no doubt that in certain areas and in specific seasons one would find intensification or deintensification. However, as the spatial scale and observation period increase, the risk for a false claim of intensification decreases. For example, in their recent study based on 1427 stations across China over the last 60 years, Wang and Sun (2020) concluded that there is no significant difference in the annual precipitations between

735   the past 20 years (1999–2018) and the past 60 years (1959–2018) and suggest to utilize the historical data of annual precipitation as the basis of water-resources application.

- We use simple and easily reproducible methodology and provide all information for reproducibility of the results. The quantities we use are observable or estimated quantities as given in the original data sets, without making any post processing or transformation (e.g., probability-based indices based on fitted distributions or regression on "signals", like in Paik et al. 2020), which could involve subjective choices.

740

- We follow Aristotle's advice (to "look for precision in each class of things just so far as the nature of the subject admits"; see the motto in the beginning). For example, an alleged 2% total increase in the precipitation over land during the entire 20th century (Huntington, 2006, and references therein) is far beyond the precision of estimating precipitation over land.

745   **Appendix B: Extremes and impacts – Does wet become wetter?**

While, as articulated in section 4, intensification of the global hydrological cycle can hardly be supported on the basis of global precipitation and evaporation fluxes, a large body of literature attempts to re-establish intensification on the basis of extremes. There is no shortage of studies that diagnosed such intensification. To refer to just one example, the results of Donat et al. (2016) and specifically those in their Figure 1 referring to the annual-maximum daily precipitation, show some increase in the

750   recent decades, which perhaps inspired their article title "More extreme precipitation in the world's dry and wet regions." However, examining their graphs, it is seen that the climatic value of annual maximum daily rainfall of the 30-year period 1980 – 2010, compared to that of 1960-80, is greater by 5% for dry areas and by 2% for wet areas. These percentages may perhaps be not meaningful to a hydrologist who deals with real-world planning and design. Also specifying particular areas such as dry and wet (which are subjectively defined and in the above study represent a small portion of the globe) and

755   neglecting others, may distort the entire global picture.

Extremes are connected to disasters. Shortage of disasters has never been the case but our perception on them is driven less by disasters per se and more by their communication. In this respect, one may notice increasing trends both on reporting disasters to the general public and on production of research articles on disasters. Such articles typically focus on particular areas recently hit by disasters. California is a popular example, but not the only one. Evidently, if we choose at random, say,

760   12 000 sites on earth, then every month we will have, on the average, one catastrophic event of a thousand-year return period in one of the sites. The roots of intensification of disaster reporting belong to the domains of psychology (cf. the notion of *availability bias*) and sociology rather than of hydrology. Thus, Blöschl and Montanari (2010) note:

There may also be a sociological element to the interpretation of flood trends which we term as the hydrologist's paradox: A recent large flood in a catchment will often lead to funding a study on the flood history of that catchment

765   *which will find there was a large flood at the end of the record. Simultaneously analysing many catchments in a large region will help reduce the chances of these self-fulfilling prophesies.*

This social behaviour of targeting research to recent disasters, which however lose societal focus after some time, has been also known the *hydro-illogical cycle*, a term attributed to Vit Klemes (Kundzewicz et al., 1993) but perhaps used earlier by others (Anderson et al., 1977).

770   As a result of intensification of disaster reporting, people think that rainfall events have become more intense or frequent recently. However, based on a list of world record point precipitation measurements compiled by Koutsoyiannis and Papalexiou (2017) for various time scales ranging from 1 min to 2 years, the fact is that the highest frequency of record rainfall events occurred in the period 1960-80; later the frequency was decreased remarkably.

775   A more detailed analysis can be based on the four sources of daily rainfall information analysed here. This analysis has been performed separately for each continent and its results are presented graphically. Figure B1 shows the temporal evolution of the monthly maximum daily precipitation areally averaged over the continents. Figure B2 shows similar information but for the areally maximum, over each continent, monthly maximum daily precipitation. None of the figures in none of the continents and none of the sources of data provides support on the intensification allegation. In particular, the observational data (CPC and GPCP) could support the opposite hypothesis, that of extreme rainfall deintensification. This becomes even more evident

780   if we examine the temporal evolution of standard deviation of daily precipitation in each month, averaged over land. In this respect, Figure B3, shows that deintensification, expressed as decreasing standard deviation, is evident in the 21st century both from CPC and GPCP observational data. This confirms an earlier result by Sun et al. (2012) who, using global land-based (2.5°×2.5°) observations in seven monthly databases, "Unexpectedly […] found a reduction in global land [precipitation] variance" and concluded that "on average, the dry became wetter while wet became drier". A similar result is shown in a

785   different manner in Figure B4 in terms of precipitation rate exceeding a threshold. Clearly, neither the frequency of high precipitation nor the sum of high intensity precipitation is intensifying. Rather, in most of the cases, there has been deintensification in the 21st century. Again, however, it will be more prudent to speak about fluctuations rather deintensification. This confirms that stationary models (but with appropriate dependence structure; see section 6.3) should also be used for extremes, as also pointed out by De Luca et al. (2020).

790   Even if there were intensification on climatic basis in percentages like 1% or 5% mentioned above, casting catastrophic prophesies about the future, would be a misleading approach. The real data on impacts of disasters of climatic type suggest spectacular drop in the severest of them since the beginning of the 20th century. Figure B5 summarizes relevant information for victims of natural disasters. The sources of data are seen Table 1 (entries 22 and 23). The climate related victims (particularly those from floods and droughts) have been diminished, while other types of disasters such as earthquakes still

795   cause large numbers of victims. Obviously, the reason behind such diminishing is not that floods and droughts have become less severe or less frequent. Rather it is the fact that in the 20th century, instead of casting pessimistic prophesies about the future, the societies improved hydrotechnology, water management, and risk assessment and reduction, while strengthening the international collaboration and the economy, so that the advances could be actually implemented.

Acknowledgments. I am grateful to the colleagues who have put online their huge data sets, as well as the data processing systems they developed. This has been the most important development in hydrology and geophysics since the time I entered academia several decades ago, to which I too have consistently tried to contribute in my country, with only partial success. I have started this research on the occasion of four invited lectures and seminars during 2017-19 in Lunz, Palermo, Moscow and Bologna (eventually cancelled).

I thank the colleagues who invited me or were involved in any respect with the organization of the talks: Dario Braga, Alexander Gelfan, Tatiana Fyodorova, Elisabet Ejarque Gonzalez, Goffredo La Loggia, Alberto Montanari, Valerio Noto, Dimitri Solomatine, Tz-Ching Yeh. I wish to clarify that my acknowledgment and thanks to them are not meant to imply that they agree with my opinions. I also thank an Austrian professor unknown to me, Rafael Bras, and James Kirchner, who by their strongly negative reactions during my lectures in Lunz, Palermo and Moscow, respectively, helped me to strengthen my analyses and results. The Italian newspaper *La Repubblica* and a blog it hosts, by their ad hominem attack with fake "information" and by baptizing me "negazionista" ("denier"), helped cancel my lecture in Bologna, which gave me the occasion to write up this material into a journal article, as well as to penetrate into relevant sociological, historical and philosophical issues. I thank the eponymous reviewers Zbigniew W. Kundzewicz (2020) and Axel Kleidon (2020) for their time and effort to provide reviews for my paper. I also thank those who contributed in external discussions of the paper, and particularly Andrew Montford and John Robson for compiling summaries of my paper.

Finally, I thank Stavros Alexandris, Ken B. Gregory, Alberto Montanari, Roger Pielke Sr., Geoff Smith, Richard Vogel and Peili Wu, for their emails with corrections and suggestions. Again, my thanks to them are not meant to imply that they agree with my opinions.

Funding. The author received no funding for this research.

Data availability. All data used in the study are freely available as described in the article and in particular in Table 1, which provides all required links.

References

Acker, J.G., and Leptoukh, G.: Online analysis enhances use of NASA earth science data, Eos, Trans. AGU, 88 (2), 14&17, 2007.

Adler, R., Wang, J.-J., Sapiano, M., Huffman, G., Chiu, L., Xie, P.P., Ferraro, R., Schneider, U., Becker, A., Bolvin, D., Nelkin, E., Gu, G., and NOAA CDR Program: Global Precipitation Climatology Project (GPCP) Climate Data Record (CDR), Version 2.3 (Monthly). National Centers for Environmental Information, doi: 10.7289/V56971M6, 2016.

Adler, R., Wang, J.-J., Sapiano, M., Huffman, G., Bolvin, D., Nelkin, E., and NOAA CDR Program: Global Precipitation Climatology Project (GPCP) Climate Data Record (CDR), Version 1.3 (Daily). NOAA National Centers for Environmental Information. doi: 10.7289/V5RX998Z, 2017.

Anagnostopoulos, G.G., Koutsoyiannis, D., Christofides, A., Efstratiadis, A., and Mamassis, N.: A comparison of local and aggregated climate model outputs with observed data, Hydrological Sciences Journal, 55 (7), 1094–1110, doi: 10.1080/02626667.2010.513518, 2010.

Anderson, J.W., DeRemer, C.W. and Hall, R.S.: Water use and management in an arid region: Fort Collins, Colorado, and vicinity. Information series (Colorado Water Resources Research Institute); no. 26. https://mountainscholar.org/bitstream/handle/10217/3085/is_26.pdf?sequence=1 (accessed February 2020), 1977.

Archfield, S.A., Clark, M., Arheimer, B., Hay, L.E., McMillan, H. et al.: Accelerating advances in continental domain hydrologic modelling, Water Resour. Res. 51 (12), 10078-10091, doi: 10.1002/2015WR017498, 2015.

Bierkens, M.F.P., and Wada, Y.: Non-renewable groundwater use and groundwater depletion: a review, Environ. Res. Lett. 14 063002, doi: 10.1088/1748-9326/ab1a5f, 2019.

Blöschl, G., and Montanari, A: Climate change impacts—throwing the dice?. Hydrological Processes, 24 (3), 374-381, 2010.

Bridgman, P.W.: The Way Things Are, Harvard University Press, 1966.

Burgess, M.G., Ritchie, J., Shapland, J. and Pielke Jr, R.: IPCC baseline scenarios over-project CO_2 emissions and economic growth, SocArXiv, doi: 10.31235/osf.io/ahsxw, 2020.

Chao, B.F., Wu, Y.H., and Li, Y.S.: Impact of artificial reservoir water impoundment on global sea level, Science, 320 (5873), 212-214, 2008.

Chen, C., Park, T., Wang, X., Piao, S., Xu, B., Chaturvedi, R.K., Fuchs, R., Brovkin, V., Ciais, P., Fensholt, R. and Tømmervik, H.: China and India lead in greening of the world through land-use management, Nature Sustainability, 2 (2), 122-129, 2019.

Chen, J.L., Pekker, T., Wilson, C.R., Tapley, B.D. Kostianoy, A.G. Cretaux, J.-F. and Safarov E.S.: Long-term Caspian Sea level change, Geophys. Res. Lett., 44, 6993–7001, doi: 10.1002/2017GL073958, 2017.

Christy, J.R., Norris, W.B., Spencer, R.W., and Hnilo, J.J.: Tropospheric temperature change since 1979 from tropical radiosonde and satellite measurements, Journal of Geophysical Research, 112, D06102, doi:10.1029/2005JD006881, 2007.

Church, T.M.: An underground route for the water cycle, Nature, 380 (6575), 579-580, 1996.

Copernicus Climate Change Service: ERA5: Fifth generation of ECMWF atmospheric reanalyses of the global climate, Copernicus Climate Change Service Climate Data Store (CDS), https://cds.climate.copernicus.eu/cdsapp#!/home (accessed January 2020), 2017.

Creed I.F., Hwang, T., Lutz, B., and Way, D.: Climate warming causes intensification of the hydrological cycle, resulting in changes to the vernal and autumnal windows in a northern temperate forest. Hydrol. Process. doi: 10.1002/hyp.10450, 2015.

860 Cretaux J.F., Kostianoy A., Bergé-Nguyen, M., and Kouraev A.: Present-Day Water Balance of the Aral Sea Seen from Satellite. In: Barale V., Gade M. (eds) Remote Sensing of the Asian Seas. doi: 10.1007/978-3-319-94067-0_29, Springer, Cham, Switzerland, 2019.

Dai, A.: Historical and future changes in streamflow and continental runoff: A review, Chapter 2 in Tang, Q., and Oki, T. (eds.), Terrestrial Water Cycle and Climate Change: Natural and Human-Induced Impacts, Geophysical Monograph 221, edited by AGU, John Wiley & Sons, 17-37, 2016.

865 Dai, A., and Trenberth, K.E.: Estimates of freshwater discharge from continents: Latitudinal and seasonal variations, Journal of Hydrometeorology, 3 (6), 660–687, 2002.

De Luca D.L., Petroselli A., and Galasso L.: Modelling climate changes with stationary models: Is it possible or is it a paradox?, in: Sergeyev Y., and Kvasov D. (eds) Numerical Computations: Theory and Algorithms, NUMTA 2019, Lecture Notes in Computer Science, 11974. Springer, Cham, Switzerland, 2020.

870 Déry, S J., Hernández-Henríquez, M.A., Burford, J.E., and Wood, E.F.: Observational evidence of an intensifying hydrological cycle in northern Canada, Geophysical Research Letters, 36, L13402, doi: 10.1029/2009GL038852, 2009.

Dingman, S.L., Physical Hydrology, Prentice Hall, Englewood Cliffs, New Jersey, 1994.

Donat, M.G., Lowry, A.L., Alexander, L.V., O'Gorman, P.A., and Maher, N.: More extreme precipitation in the world's dry and wet regions, Nature Climate Change, 6, doi: 10.1038/NCLIMATE2941, 2016.

875 Eicker, A., Forootan, E., Springer, A., Longuevergne, L., and Kusche, J.: Does GRACE see the terrestrial water cycle "intensifying"?, J. Geophys. Res. Atmos., 121, 733–745, doi: 10.1002/2015JD023808, 2016.

Estilow, T.W., Young, A.H., and Robinson, D.A.: A long-term Northern Hemisphere snow cover extent data record for climate studies and monitoring, Earth Syst. Sci. Data, 7, 137–142, doi: 10.5194/essd-7-137-2015, 2015.

Fleming, K., Johnston, P., Zwartz, D., Yokoyama, Y., Lambeck, K., and Chappell, J.: Refining the eustatic sea-level curve
880 since the Last Glacial Maximum using far- and intermediate-field sites, Earth and Planetary Science Letters, 163 (1-4): 327-342. doi:10.1016/S0012-821X(98)00198-8, 1998.

Gardner, A.S., Moholdt, G., Cogley, J.G., Wouters, B., Arendt, A.A., Wahr, J., Berthier, E., Hock, R., Pfeffer, W.T., Kaser, G. and Ligtenberg, S.R.: A reconciled estimate of glacier contributions to sea level rise: 2003 to 2009, Science, 340 (6134), 852-857. 2013.

885 Gaybullaev, B., Chen, S. and Gaybullaev, D.: Changes in water volume of the Aral Sea after 1960, Appl. Water Sci., 2, 285–291, doi: 10.1007/s13201-012-0048-z, 2012.

Ghiggi, G., Humphrey, V., Seneviratne, S.I. and Gudmundsson, L.: GRUN: an observation-based global gridded runoff dataset from 1902 to 2014, Earth System Science Data, 11 (4), 1655-1674, 2019.

890 Gloor, M., Brienen, R.J.W., Galbraith, D., Feldpausch, T.R., Schöngart, J., Guyot, J.-L., Espinoza, J.C., Lloyd, J., and Phillips, O.L.: Intensification of the Amazon hydrological cycle over the last two decades, Geophysical Research Letters, 40, 1729–1733, doi: 10.1002/grl.50377, 2013.

Hallam, A.: Pre-Quaternary sea-level changes, Annu. Rev. Earth Planet. Sci. 12, 205–243, doi: 10.1146/annurev.ea.12.050184.001225, 1984.

Hanna, E., Pattyn, F., Navarro, F., Favier, V., Goelzer, H., van den Broeke, M.R., Vizcaino, M., Whitehouse, P.L., Ritz, C., 895 Bulthuis, K., and Smith, B. Mass balance of the ice sheets and glaciers – Progress since AR5 and challenges, Earth-Science Reviews,, 201, doi: 10.1016/j.earscirev.2019.102976, 2020.

Hersbach, H., and Dee, D.: ERA5 reanalysis is in production, ECMWF Newsletter, 147 (7), 5-6, 2016.

Hubanks, P., Platnick, S., King, M., and Ridway, B.: MODIS Atmosphere L3 Gridded Product Algorithm Theoretical Basis Document (ATBD) & Users Guide (Collection 006, Version 4.1, 22 September 2015), http://icdc.cen.uni-900 hamburg.de/fileadmin/user_upload/icdc_Dokumente/MODIS/MODIS_Collection6_AtmosphereL3_GriddedProduct_ATBD andUsersGuide_v4.1_Sep22_2015.pdf (accessed February 2020), 2015.

Huffman, G.J., Adler, R.F., Morrissey, M., Bolvin, D.T., Curtis, S., Joyce, R., McGavock, B., and Susskind, J.: Global precipitation at one-degree daily resolution from multi-satellite observations. J. Hydrometeor., 2 (1), 36-50, 2001.

Huntington, T.G.: Evidence for intensification of the global water cycle: Review and synthesis, Journal of Hydrology 319 (1–905 4), 83-95 doi: 10.1016/j.jhydrol.2005.07.003, 2006.

Hurst, H.E.: Long term storage capacities of reservoirs. *Trans. Am. Soc. Civil Eng.*, 116, 776–808, 1951.

Iliopoulou, T., and Koutsoyiannis, D: Projecting the future of rainfall extremes: better classic than trendy, Journal of Hydrology, 558, Article 125005, doi: 10.1016/j.jhydrol.2020.125005, 2020.

IMBIE (Shepherd, A., Ivins, E., Rignot, E. et al.): Mass balance of the Antarctic Ice Sheet from 1992 to 2017, Nature 558, 910 219–222 10.1038/s41586-018-0179-y, 2018.

IMBIE (Shepherd, A., Ivins, E., Rignot, E. et al.): Mass balance of the Greenland Ice Sheet from 1992 to 2018, Nature 579, 233–239, doi: 10.1038/s41586-019-1855-2, 2020.

IPCC: Climate Change 2013: The Physical Science Basis. Contribution of Working Group I to the Fifth Assessment Report of the Intergovernmental Panel on Climate Change. Cambridge University Press, Cambridge, UK and New York, NY, 1535 915 pp. http://www.climatechange2013.org/report/ (accessed 2020-02-14), 2013.

Kalnay, E., Kanamitsu, M., Kistler, R., Collins, W., Deaven, D., Gandin, L., Iredell, M., Saha, S., White, G., Woollen, J. and Zhu, Y.: The NCEP/NCAR 40-year reanalysis project, Bulletin of the American Meteorological Society, 77 (3), 437-472, 1996.

Khedun, C.P., and Singh, V.P.: Water balance, Ch. 3 in Singh, V.P. (ed.) Handbook of Applied Hydrology, Second Edition, 920   3.1–3.11, McGraw-Hill, New York, 2017.

Kleidon, A. and Renner, M.: A simple explanation for the sensitivity of the hydrologic cycle to surface temperature and solar radiation and its implications for global climate change, Earth Syst. Dynam., 4, 455–465, doi: 10.5194/esd-4-455-2013, 2013.

Kleidon, A.: Interactive comment on "Revisiting global hydrological cycle: Is it intensifying?" by Demetris Koutsoyiannis, Hydrol. Earth Syst. Sci. Discuss., doi: 10.5194/hess-2020-120-RC2, 2020.

925   Kleidon, A., Kravitz, B., and M. Renner, M.: The hydrological sensitivity to global warming and solar geoengineering derived from thermodynamic constraints, Geophys. Res. Lett., 42, 138–144, doi: 10.1002/2014GL062589, 2015.

Kolmogorov, A.N.: Wiener spirals and some other interesting curves in a Hilbert space. Dokl. Akad. Nauk SSSR, 26, 115-118. (English edition: Kolmogorov, A.N., 1991, Selected Works of A. N. Kolmogorov - Volume 1, Mathematics and Mechanics, ed. by Tikhomirov, V.M., Kluwer, Dordrecht, The Netherlands,, 324-326). 1940

930   Koutsoyiannis, D.: HESS Opinions "A random walk on water", Hydrology and Earth System Sciences, 14, 585–601, doi: 10.5194/hess-14-585-2010, 2010.

Koutsoyiannis, D.: Hurst-Kolmogorov dynamics and uncertainty, Journal of the American Water Resources Association, 47 (3), 481–495, doi: 10.1111/j.1752-1688.2011.00543.x, 2011.

Koutsoyiannis, D.: Clausius-Clapeyron equation and saturation vapour pressure: simple theory reconciled with practice, 935   European Journal of Physics, 33 (2), 295–305, doi: 10.1088/0143-0807/33/2/295, 2012.

Koutsoyiannis, D.: Hydrology and change, Hydrological Sciences Journal, 58 (6), 1177–1197, doi: 10.1080/02626667.2013.804626, 2013.

Koutsoyiannis, D.: Reconciling hydrology with engineering, Hydrology Research, 45 (1), 2–22, doi: 10.2166/nh.2013.092, 2014a.

940   Koutsoyiannis, D:. Entropy: from thermodynamics to hydrology, Entropy, 16 (3), 1287–1314, doi: 10.3390/e16031287, 2014b.

Koutsoyiannis, D:: Rebuttal to review comments on "Revisiting global hydrological cycle: Is it intensifying?" (Interactive comment on "Revisiting global hydrological cycle: Is it intensifying?" by Demetris Koutsoyiannis), Hydrol. Earth Syst. Sci. Discuss., doi: 10.5194/hess-2020-120-AC1, 2020a.

945 Koutsoyiannis, D:: Appendix to Rebuttal to review comments on "Revisiting global hydrological cycle: Is it intensifying?" (Interactive comment on "Revisiting global hydrological cycle: Is it intensifying?" by Demetris Koutsoyiannis), Hydrol. Earth Syst. Sci. Discuss., doi: 10.5194/hess-2020-120-AC2, 2020b.

Koutsoyiannis, D. Christofides, A., Efstratiadis, A., Anagnostopoulos, G.G., and Mamassis, N.: Scientific dialogue on climate: is it giving black eyes or opening closed eyes? Reply to "A black eye for the Hydrological Sciences Journal" by D. Huard, Hydrological Sciences Journal, 56 (7), 1334–1339, doi: 10.1080/02626667.2011.610759, 2011.

950 Koutsoyiannis, D. Efstratiadis, A., Mamassis, N., and Christofides, A.: On the credibility of climate predictions. Hydrological Sciences Journal, 53 (4), 671–684, doi: 10.1623/hysj.53.4.671, 2008.

Koutsoyiannis, D., and Montanari, A.: Statistical analysis of hydroclimatic time series: Uncertainty and insights, Water Resources Research, 43 (5), W05429, doi: 10.1029/2006WR005592, 2007.

Koutsoyiannis, D., and Montanari, A.: Negligent killing of scientific concepts: the stationarity case, Hydrological Sciences 955 Journal, 60 (7-8), 1174–1183, doi: 10.1080/02626667.2014.959959, 2015.

Koutsoyiannis, D., Montanari, A., Lins, H.F., and Cohn, T.A.: Climate, hydrology and freshwater: towards an interactive incorporation of hydrological experience into climate research—DISCUSSION of "The implications of projected climate change for freshwater resources and their management", Hydrological Sciences Journal, 54 (2), 394–405, doi: 10.1623/hysj.54.2.394, 2009.

960 Koutsoyiannis, D. and Papalexiou, S.M.: Extreme rainfall: Global perspective, Ch. 74 in Singh, V.P. (ed.) Handbook of Applied Hydrology, Second Edition, 74.1–74.16, McGraw-Hill, New York, 2017.

Kundzewicz Z.W.: Interactive comment on "Revisiting global hydrological cycle: Is it intensifying?" by Demetris Koutsoyiannis, Hydrol. Earth Syst. Sci. Discuss., doi: 10.5194/hess-2020-120-RC1, 2020.

Kundzewicz, Z.W., Rosbjerg, D., Simonovic, S.P., and Takeuch, K.: Extreme hydrological events: Precipitation, Floods and 965 droughts, Proceedings of the Yokohama Symposium, July 1993, IAHS Publ. no. 213, http://hydrologie.org/redbooks/a213/iahs_213_0001.pdf (accessed February 2020), 1993.

Kundzewicz, Z.W., and Stakhiv, E.Z.: Are climate models "ready for prime time" in water resources management applications, or is more research needed?, Hydrological Sciences Journal, 55 (7), 1085-1089, doi: 10.1080/02626667.2010.513211, 2010.

Llovel, W., Willis, J., Landerer, F. and Fukumori, I.: Deep-ocean contribution to sea level and energy budget not detectable 970 over the past decade. Nature Clim Change 4, 1031–1035, doi: 10.1038/nclimate2387, 2014.

Lvovitch, M.I.: World water balance (general report), in: World water balance: Proceedings of the Reading Symposium, IASH-UNESCO-WMO, 1970, Vol. II (Publ., 93), 401-415, http://hydrologie.org/redbooks/a092/093019.pdf (accessed February 2020), 1970.

Madakumbura, G.D., Kim, H., Utsumi, N., Shiogama, H., Fischer, E.M., Seland, Ø., Scinocca, J.F., Mitchell, D.M.,
975 Hirabayashi, Y., and Oki, T.: Event-to-event intensification of the hydrologic cycle from 1.5 °C to a 2 °C warmer world,
Scientific Reports 9, Article number: 3483, doi: 10.1038/s41598-019-39936-2, 2019.

Mamassis, N., Efstratiadis, A., Dimitriadis, P., Iliopoulou, T., Ioannidis, R., and Koutsoyiannis, D.: Water and Energy, in
Handbook of Water Resources Management: Discourses, Concepts and Examples (ed. by J.J. Bogardi, K.D. Wasantha
Nandalal, R.R.P. van Nooyen, and A. Bhaduri), Springer, Cham, Switzerland, 2020.

980 Markonis, Y., and Koutsoyiannis, D.: Climatic variability over time scales spanning nine orders of magnitude: Connecting
Milankovitch cycles with Hurst–Kolmogorov dynamics, Surveys in Geophysics, 34 (2), 181–207, doi: 10.1007/s10712-012-
9208-9, 2013.

Marzeion, B., Leclercq, P.W., Cogley, J.G., and Jarosch, A.H.: Brief Communication: Global reconstructions of glacier mass
change during the 20th century are consistent, The Cryosphere, 9, 2399–2404, https://doi.org/10.5194/tc-9-2399-2015, 2015.

985 Montanari, A., and Koutsoyiannis, D.: Modeling and mitigating natural hazards: Stationarity is immortal!, Water Resources
Research, 50 (12), 9748–9756, doi: 10.1002/2014WR016092, 2014.

Nace, R.L.: Water of the World, Natural History, Vol. LXXIII, No. 1, 1964

Nace, R.L.: Are we running out of water?), US Geological Survey. No. 536, 1967.

Nace, R.L.: Groundwater: perspectives and prospects, Water Well J., 23 (2), 28-29, 1969.

990 Nace, R.L.: World hydrology: status and prospects, in: World Water Balance, Proceedings of the Reading Symposium, IASH-
UNESCO-WMO, 1970. Vol. I, Publ., 92, pp. 1-10 http://hydrologie.org/redbooks/a092/092004.pdf (accessed February 2020),
1970.

O'Connell, P.E., Koutsoyiannis, D. Lins, H.F., Markonis, Y., Montanari, A., and Cohn, T.A.: The scientific legacy of Harold
Edwin Hurst (1880 – 1978), Hydrological Sciences Journal, 61 (9), 1571–1590, doi:1 0.1080/02626667.2015.1125998, 2016.

995 Oki, T. and Kanae, S.: Global hydrological cycles and world water resources, Science, 313 (5790), 1068-1072, 2006.

Paik, S., Min, S.-K., Zhang, X., Donat, M.G., King, A.D., and Sun, Q.: Determining the anthropogenic greenhouse gas
contribution to the observed intensification of extreme precipitation. Geophysical Research Letters, 47, e2019GL086875, doi:
10.1029/2019GL086875, 2020.

Pielke Sr, R.A., Mahmood, R. and McAlpine, C.: Land's complex role in climate change, Physics Today, 69(11), 40, doi:
1000 10.1063/PT.3.3364, 2016.

Platnick, S., et al.: MODIS Atmosphere L3 Monthly Product, NASA MODIS Adaptive Processing System, Goddard Space
Flight Center, USA, doi: 10.5067/MODIS/MOD08_M3.006 and 10.5067/MODIS/MYD08_M3.006, 2015.

Robinson, D.A., Estilow, T.W., and NOAA CDR Program: NOAA Climate Data Record (CDR) of Northern Hemisphere (NH) Snow Cover Extent (SCE), Version 1. NOAA National Centers for Environmental Information. doi: 10.7289/V5N014G9, 2012.

Schellekens, J., Dutra, E., la Torre, A.M.D., Balsamo, G., van Dijk, A., Weiland, F.S., Minvielle, M., Calvet, J.C., Decharme, B., Eisner, S., Fink, G.,Flörke, M., Peßenteiner, S., van Beek, R., Polcher, J., Beck, H., Orth, R., Calton, B., Burke, S., Dorigo, W., and Weedon, G.P.: A global water resources ensemble of hydrological models: The eartH2Observe Tier-1 dataset, Earth System Science Data, 9, 389-413, 2017.

Seidel, S.D., and Yang, D.: The lightness of water vapor helps to stabilize tropical climate, Science Advances, 6 (19), doi: 10.1126/sciadv.aba1951, 2020.

Shiklomanov, I.A. and Sokolov, A.A.: Methodological basis of world water balance investigation and computation. IAHS publication 148, 77-92, http://hydrologie.org/redbooks/a148/iahs_148_0077.pdf (accessed February 2020), 1985.

Smith, C.A., Compo, G.P., and Hooper, D.K.: Web-based Reanalysis Intercomparison Tools (WRIT) for analysis and comparison of reanalyses and other datasets, Bull. Am. Meteorol. Soc., 95 (11), 1671-1678, doi:10.1175/BAMS-D-13-00192.1, 2014.

Spencer, R.W. and Christy, J.R.: Precise monitoring of global temperature trends from satellites. Science, 247 (4950), 1558-1562, 1990.

Stephens, G.L., L'Ecuyer, T., Forbes, R., Gettelmen, A., Golaz, J.-C., Bodas-Salcedo, A., Suzuki, K., Gabriel, P., and Haynes, J.: Dreary state of precipitation in global models, J. Geophys. Res., 115, D24211, doi: 10.1029/2010JD014532, 2010.

Su, L., Miao, C., Kong, D., Duan, Q., Lei, X., Hou, Q., and Li, H.: Long-term trends in global river flow and the causal relationships between river flow and ocean signals, Journal of Hydrology, 563, 818-833, doi: 10.1016/j.jhydrol.2018.06.058, 2018.

Sun, F., Roderick, M.L., and Farquhar, G.D.: Changes in the variability of global land precipitation, Geophys. Res. Lett., 39, L19402, doi:10.1029/2012GL053369, 2012.

Syed, T.H., Famiglietti, J.S., and Chambers, D.P.: GRACE-based estimates of terrestrial freshwater discharge from basin to continental scales, Journal of Hydrometeorology, 10(1), 22-40, 2009.

Trenberth, K.E., Fasullo, J., and Smith, L.: Trends and variability in column-integrated atmospheric water vapor. Climate Dynamics 24, 741–758, doi: 10.1007/s00382-005-0017-4, 2005.

Trenberth, K.E., Fasullo, J.T., and Kiehl, J.: Earth's global energy budget, Bulletin of the American Meteorological Society, 90, 311–324, doi: 10.1175/2008BAMS2634.1, 2009.

Tsaknias, D., Bouziotas, D., and Koutsoyiannis, D.: Statistical comparison of observed temperature and rainfall extremes with climate model outputs in the Mediterranean region, ResearchGate, doi: 10.13140/RG.2.2.11993.93281, 2016.

Tyralis, H., and, Koutsoyiannis, D.: On the prediction of persistent processes using the output of deterministic models, Hydrological Sciences Journal, 62 (13), 2083–2102, doi: 10.1080/02626667.2017.1361535, 2017.

van der Meer, D.G., van den Berg van Saparoea, A.P.H., van Hinsbergen, D.J.J., van de Weg, R.M.B., Godderis, Y., Le Hir, G., and Donnadieu, Y.: Reconstructing first-order changes in sea level during the Phanerozoic and Neoproterozoic using strontium isotopes, Gondwana Research, 44, 22-34, doi: 10.1016/j.gr.2016.11.002, 2017.

Velicogna, I., Sutterley, T.C., and Van Den Broeke, M.R.: Regional acceleration in ice mass loss from Greenland and Antarctica using GRACE time-variable gravity data, Geophysical Research Letters, 41(22), 8130-8137, 2014.

Velicogna, I. and Wahr, J.: Time-variable gravity observations of ice sheet mass balance: Precision and limitations of the GRACE satellite data, Geophysical Research Letters, 40 (12), 3055-3063, 2013.

Vonder Haar, T.H., Bytheway J.L., and Forsythe, J.M.: Weather and climate analyses using improved global water vapor observations, Geophys. Res. Lett., 39, L16802, doi: 10.1029/2012GL052094, 2012.

Wada, Y.: Modeling Groundwater Depletion at Regional and Global Scales: Present State and Future Prospects, Surv. Geophys., 37, 419–451, doi: 10.1007/s10712-015-9347-x, 2016.

Wada, Y., Lo, M.H., Yeh, P.J.F., Reager, J.T., Famiglietti, J.S., Wu, R.J. and Tseng, Y.H.: Fate of water pumped from underground and contributions to sea-level rise, Nature Climate Change, 6 (8), 777-780, doi: 10.1038/nclimate3001, 2016.

Wada, Y., van Beek, L.P.H., van Kempen, C.M., Reckman, J.W.T.M., Vasak, S., and Bierkens M.F.P., Global depletion of groundwater resources, Geophys. Res. Lett., 37, L20402, doi: 10.1029/2010GL044571, 2010. Wan, Z.: Collection-6 MODIS Land Surface Temperature Products, Users' Guide, ERI, University of California, Santa Barbara, https://lpdaac.usgs.gov/documents/118/MOD11_User_Guide_V6.pdf (accessed February 2020), 2013.

Wan, Z., Hook, S., and Hulley. G.: MOD11C3 MODIS/Terra Land Surface Temperature/Emissivity Monthly L3 Global 0.05Deg CMG V006, distributed by NASA EOSDIS Land Processes DAAC, doi: 10.5067/MODIS/MOD11C3.006 (Accessed 2020-02-19), 2015.

Wang, H. and Sun, F., 2020. On the Stationarity of Annual Precipitation over China (1959-2018). Journal of Hydrometeorology, 21 (5), 881–890, doi: 10.1175/JHM-D-19-0195.1, 2020.

Wang, J.-W., Wang, K., Pielke Sr., R.A., Lin, J.C., and Matsui T.: Towards a robust test on North America warming trend and precipitable water content increase, Geophys.Res. Lett., 35, L18804, doi: 10.1029/2008GL034564, 2008.

WCRP Global Sea Level Budget Group: Global sea-level budget 1993–present, Earth Syst. Sci. Data, 10, 1551–1590, doi: 10.5194/essd-10-1551-2018, 2018.

Wild, M. et al.: Combined surface solar brightening and increasing greenhouse effect support recent intensification of the global land-based hydrological cycle, Geophysical Research Letters 35, L17706, doi: 10.1029/2008GL034842, 2008.

Wu, P., Christidis, N., and Stott, P.: Anthropogenic impact on Earth's hydrological cycle, Nature Clim. Change, 3, 807–810, doi: 10.1038/nclimate1932, 2013.

Wuebbles, D.J., Easterling, D.R., Hayhoe, K., Knutson, T,. Kopp, R.E., Kossin, J.P., Kunkel, K.E., LeGrande, A.N.,, Mears, C. Sweet, W.V., Taylor, P.C., Vose, R.S., and Wehner, M.F.: Our globally changing climate, in: Wuebbles, D.J., Fahey, D.W., Hibbard, K.A., Dokken, D.J., Stewart, B.C., and Maycock T.K. (eds.), Climate Science Special Report: Fourth National Climate Assessment, Vol. I, U.S. Global Change Research Program, Washington, DC, USA, 35-72, doi: 10.7930/J08S4N35, 2017.

Xie, P.: CPC unified gauge-based analysis of global daily precipitation, 24th Conference on Hydrology https://ams.confex.com/ams/90annual/techprogram/paper_163676.htm, (accessed February 2020), 2010.

Xie, P., Yatagai, A., Chen, M., Hayasaka, T., Fukushima, Y., Liu, C., and Yang S., A gauge-based analysis of daily precipitation over East Asia, J. Hydrometeorol., 8, 607-626, 2007.

Zektser, I.S., and Dzhamalov, R.G.: Ground water discharge to the world's oceans, Nat. Resour., 17, 18-20, 1981.

Zektzer, I.S., Ivanov, V.A., and Meskheteli, A.V.: The problem of direct groundwater discharge to the seas, Journal of Hydrology, 20 (1), 1-36, 1973.

Zekster, I., and Loaiciga, H.A.: Groundwater fluxes in the global hydrologic cycle: Past, present and future, Journal of Hydrology, 144, 405–427, 1993.

Zhou, Y.Q., Sawyer, A.H., David, C.H., & Famiglietti, J.S.: Fresh submarine groundwater discharge to the near-global coast, Geophysical Research Letters, 46, 5855–5863, doi: 10.1029/2019GL082749, 2019.

Zhu, Z., Piao, S., Myneni, R.B., Huang, M., Zeng, Z., Canadell, J.G., Ciais, P., Sitch, S., Friedlingstein, P., Arneth, A. and Cao, C.: Greening of the Earth and its drivers, Nature Climate Change, 6 (8), 791-795, 2016.

Ziegler, A.D., Sheffield, J., Maurer, E.P., Nijssen, B., Wood, E.F. and Lettenmaier, D.P.: Detection of intensification in global- and continental-scale hydrological cycles: Temporal scale of evaluation, J Clim, 16, 535-547, doi: 10.1175/1520-0442(2003)016<0535:DOIIGA>2.0.CO;2, 2003.

Zwally, H.J., Li, J., Robbins, J.W., Saba, J.L., Yi, D. and Brenner, A.C.: Mass gains of the Antarctic ice sheet exceed losses, Journal of Glaciology, 61 (230), 1019-1036, 2015.

Figures

1090
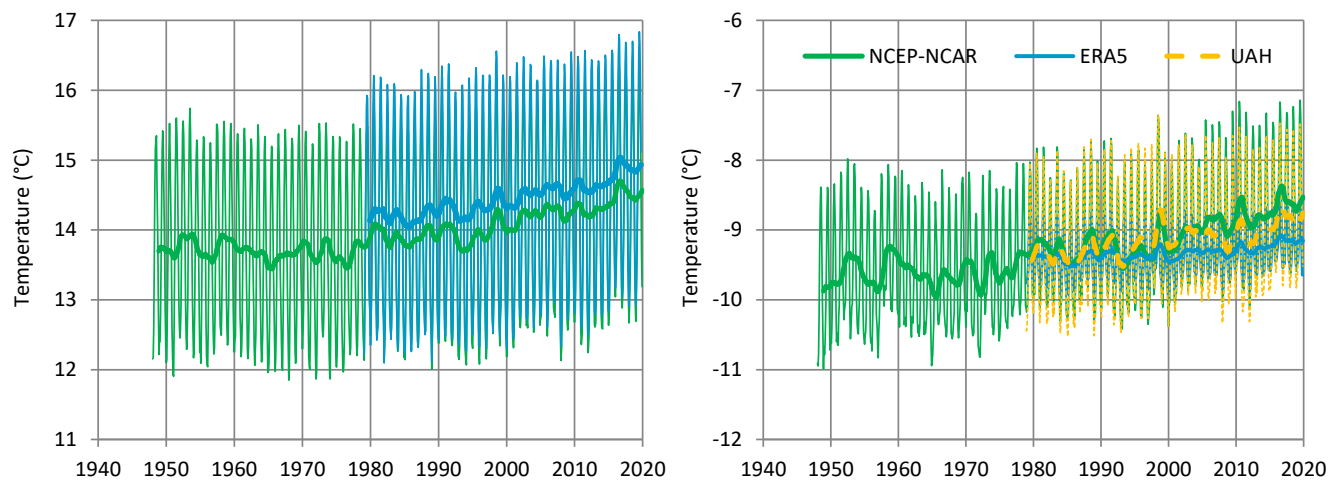
Figure 1: Variation of the global average temperature (left) at the level of 2 m above ground and (right) at the lower troposphere. Thin and thick lines of the same colour represent monthly values and running annual averages (right aligned), respectively. Sources of data are indicated in the legend and detailed in Table 1. In the right panel, the reanalyses (NCEP-NCAR and ERA5) time series are weighted averages of those at the levels of 500 and 700 hPa with weights 0.62 and 0.38, respectively, which were found for optimal
1095   **fitting with the satellite (UAH) series.**
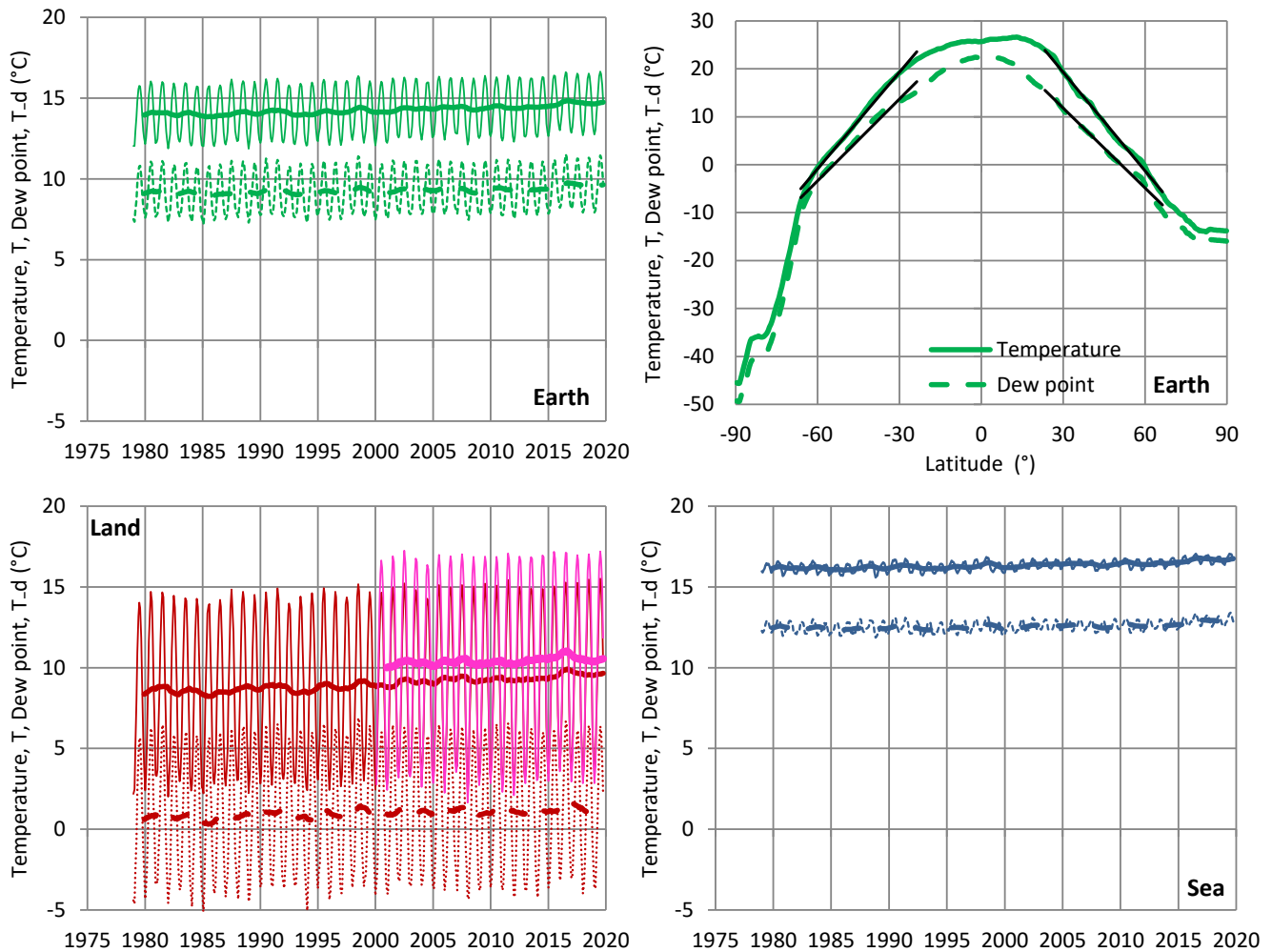
Figure 2: (Upper left) Variation of the globally averaged temperature (continuous lines) and dew point (dashed lines) at the level of 2 m above ground. Thin and thick lines of the same colour represent monthly values and running annual averages (right aligned), respectively. **(Upper right)** Zonal distribution of earth temperature and dew point; for the temperate zone (±23.5° to ±66.5°) the fitted slopes are also plotted (in black), which are ±0.68 °C/° and ±0.56 °C/°, respectively. **(Lower left and right)** As upper left but for the land and sea parts. Sources of data: ERA5 reanalysis as detailed in Table 1; for comparison and validation, in the Land graph the MODIS-terra land-surface temperature (averages of daytime and nighttime datasets, available since 2000) is also plotted in magenta.

1105
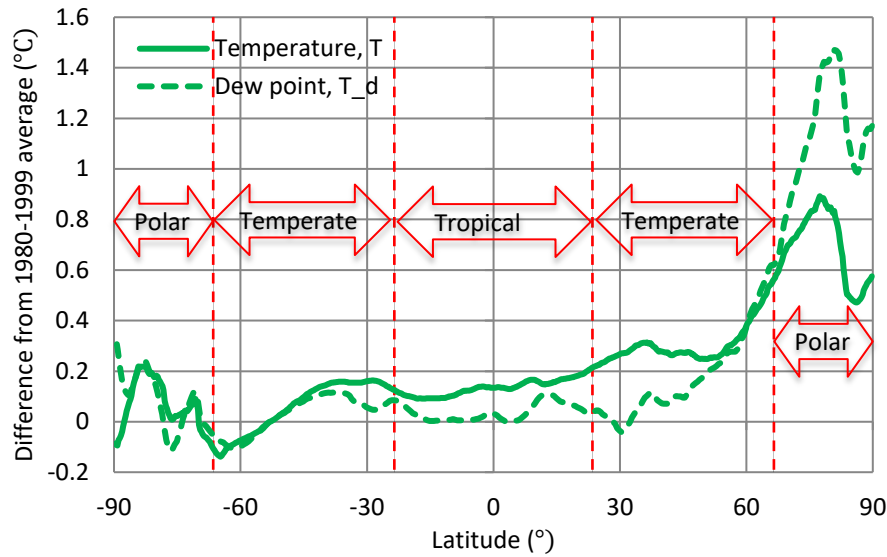
Figure 3: Zonal distribution of the difference of the earth temperature and dew point from their averages in the period 1980-99. Source of data: ERA5 reanalysis as detailed in Table 1. The data for the plot were constructed via climexp, by first computing "anomalies" for the period 1980-99, then by computing zonal mean and finally by applying the option "Compute mean, s.d., or extremes" and specifying "averaging over 12 months". Note that the graph represents averages for the entire 40+ year period, rather

1110 **than differences between two periods (the latter are about twice the former).**
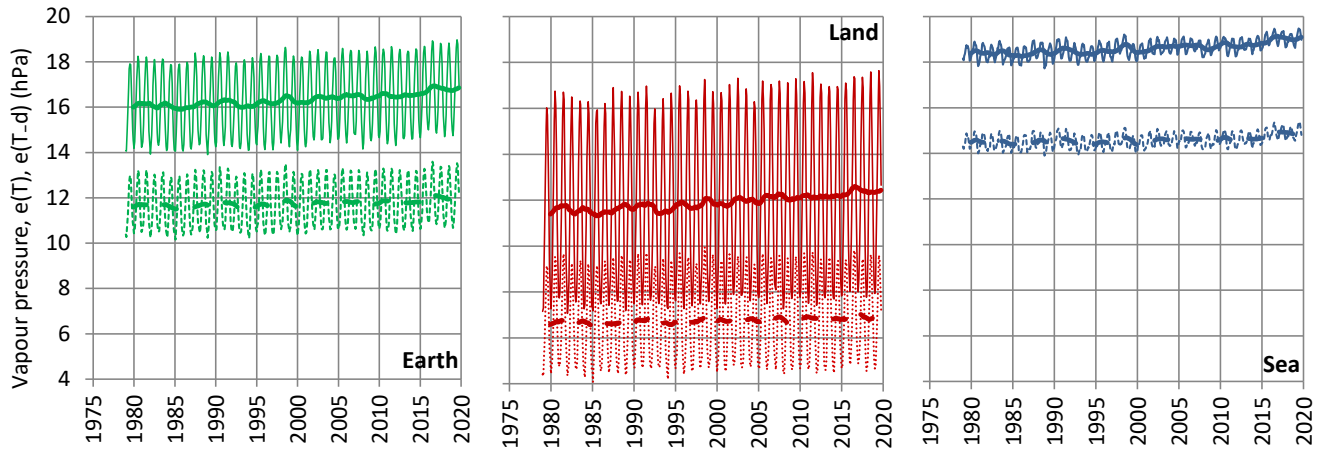
Figure 4: Variation of the saturation water pressure $e(T)$ (continuous lines) and $e(T_d)$ (dashed lines) for the average temperature T and dew point T_d as shown in Figure 2. Thin and thick lines of the same colour represent monthly values and running annual averages (right aligned), respectively. Sources of data: ERA5 reanalysis as detailed in Table 1.

1115
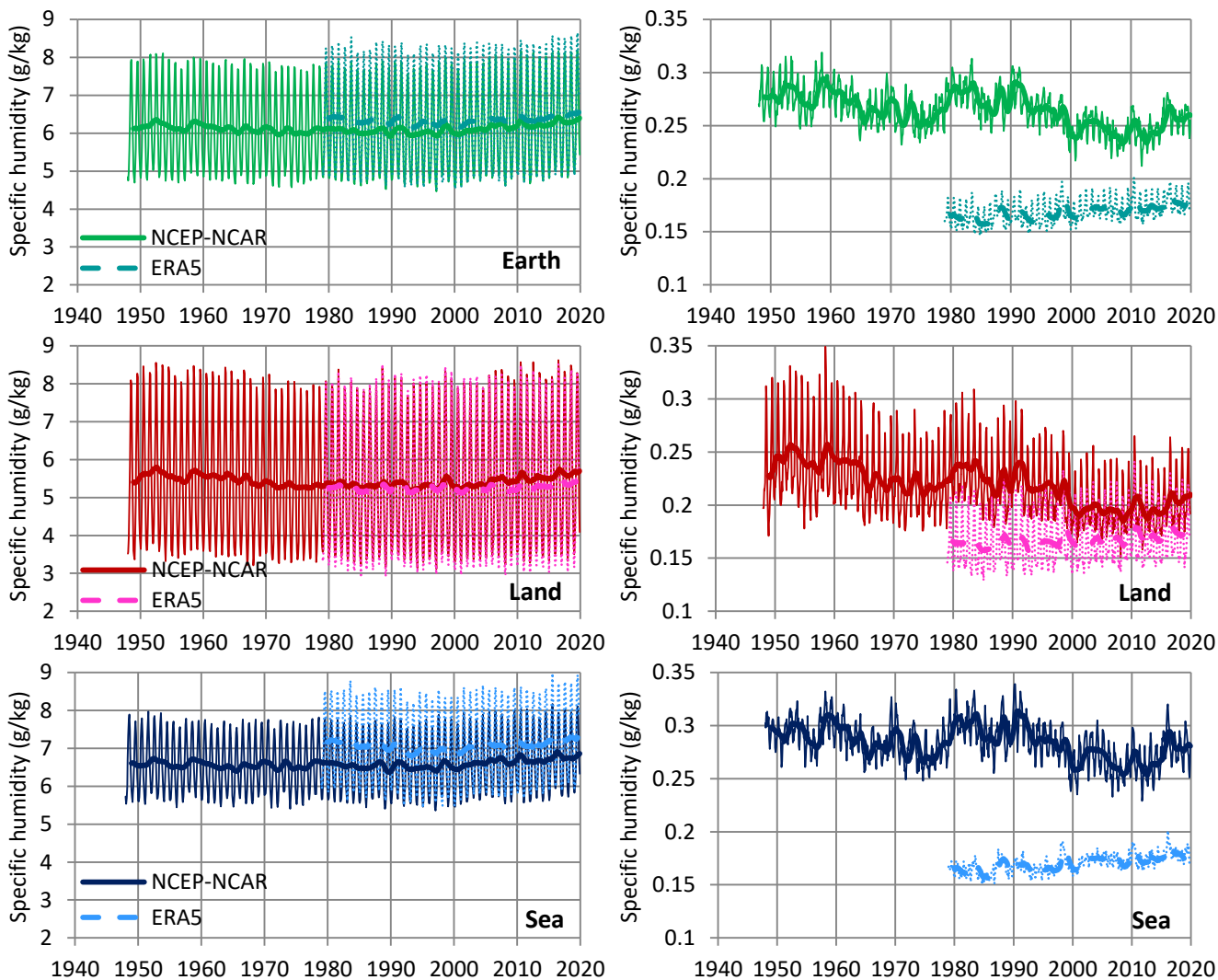
Figure 5: Variation of specific humidity at the levels of (left column) 850 hPa and (right column) 300 hPa. Thin and thick lines of the same colour represent monthly values and running annual averages (right aligned), respectively. Sources of data are indicated in the legend and detailed in Table 1.
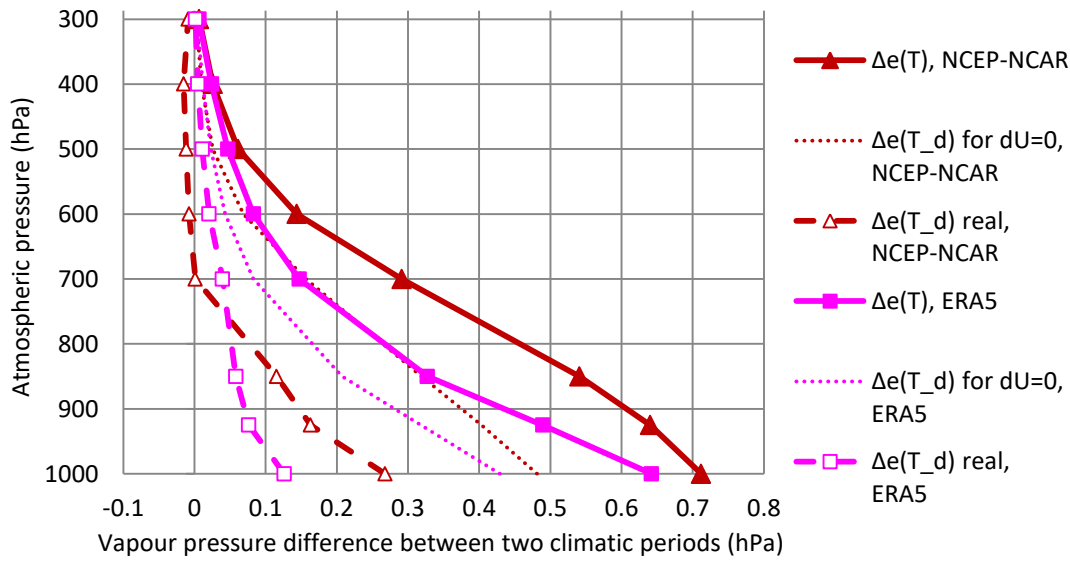
1120 **Figure 6: Vertical profile of the difference between two climatic periods of average water vapour water pressure $e(T)$ and $e(T_d) = U\,e(T)$ over land at levels of atmospheric pressure ranging from 1000 to 300 hPa. Sources of data: NCEP-NCAR and ERA5 reanalyses as detailed in Table 1 (entries 3, 4, 6, 7). For the NCEP-NCAR data, the differences are of the 30-year climatic periods 1948-77 and 1990-2019 and for the ERA5 data of the 20-year climatic periods 1980-99 and 2000-19.**
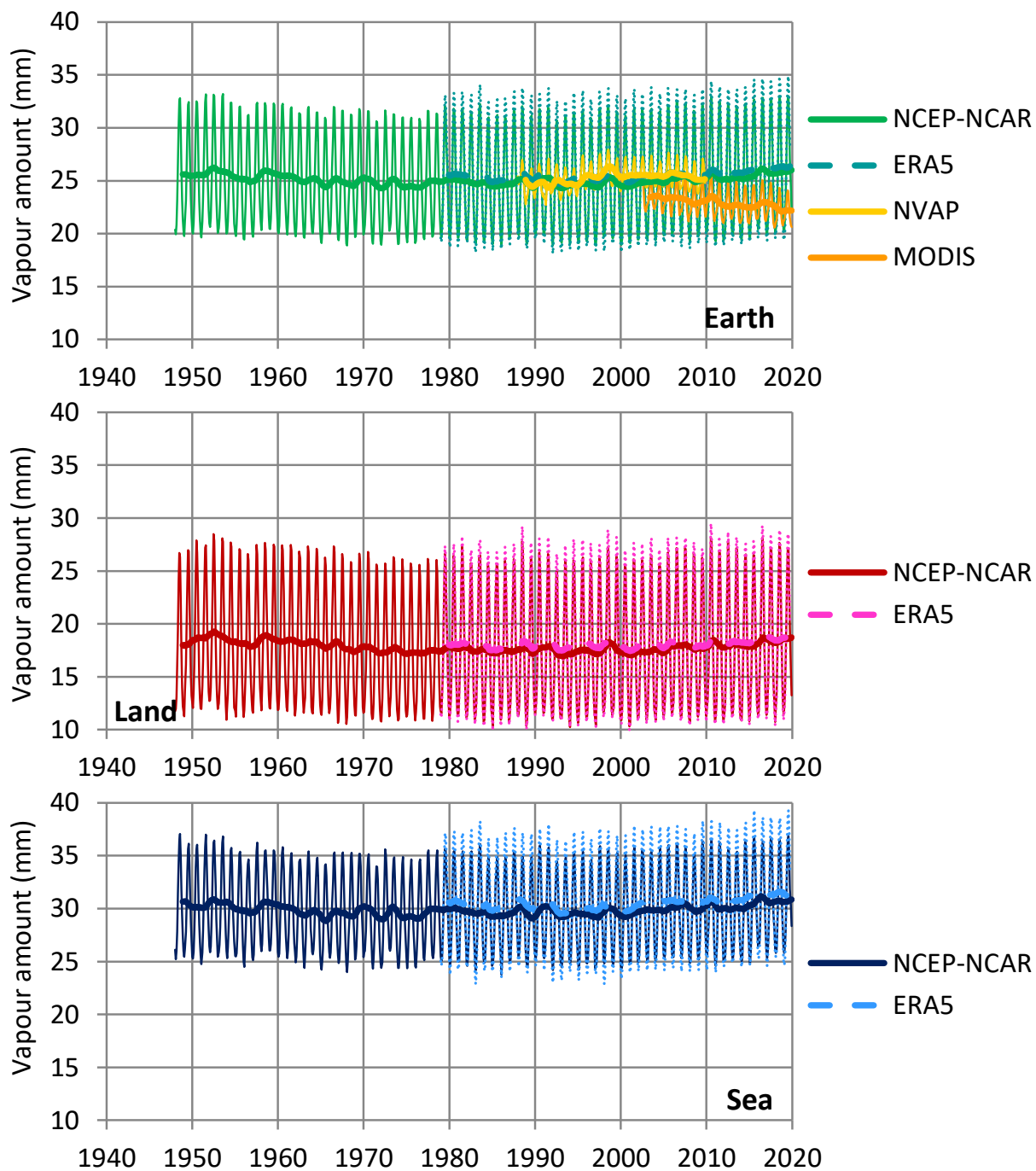
1125   **Figure 7: Variation of water vapour amount. Thin and thick lines of the same colour represent monthly values and running annual averages (right aligned), respectively. Sources of data are indicated in the legend and detailed in Table 1. The plotted values for MODIS represent the averages from Terra and Aqua platforms.**
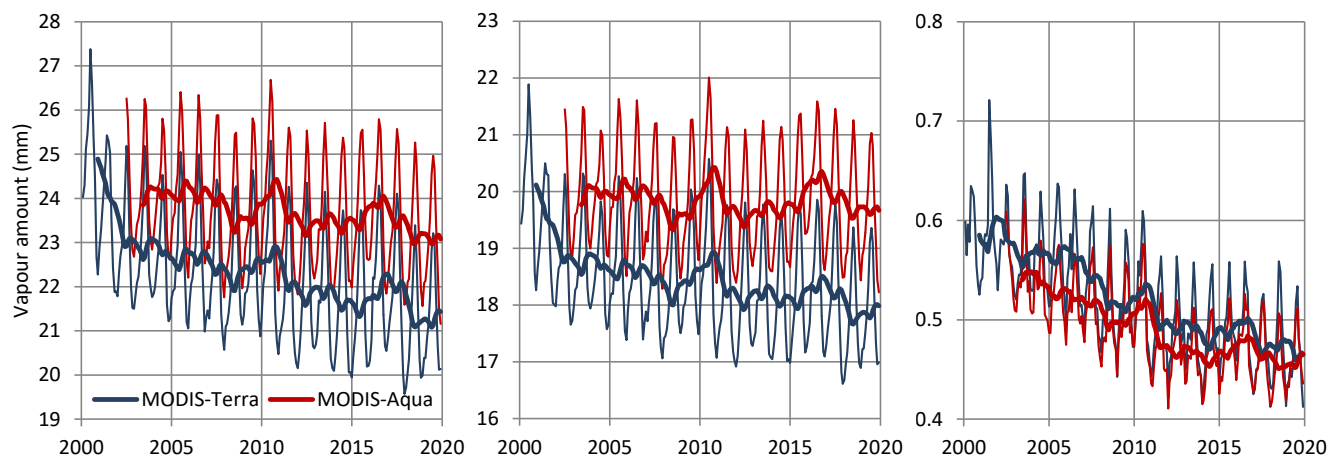
Figure 8: Variation of water vapour amount as in Figure 7 but only for the MODIS data set and separately for the Terra and Aqua platforms: (left) total of the vertical column; (middle) from surface to 680 hPa; (right) from 440 to 10 hPa. Thin and thick lines of the same colour represent monthly values and running annual averages (right aligned), respectively. Sources of data are indicated in the legend and detailed in Table 1.
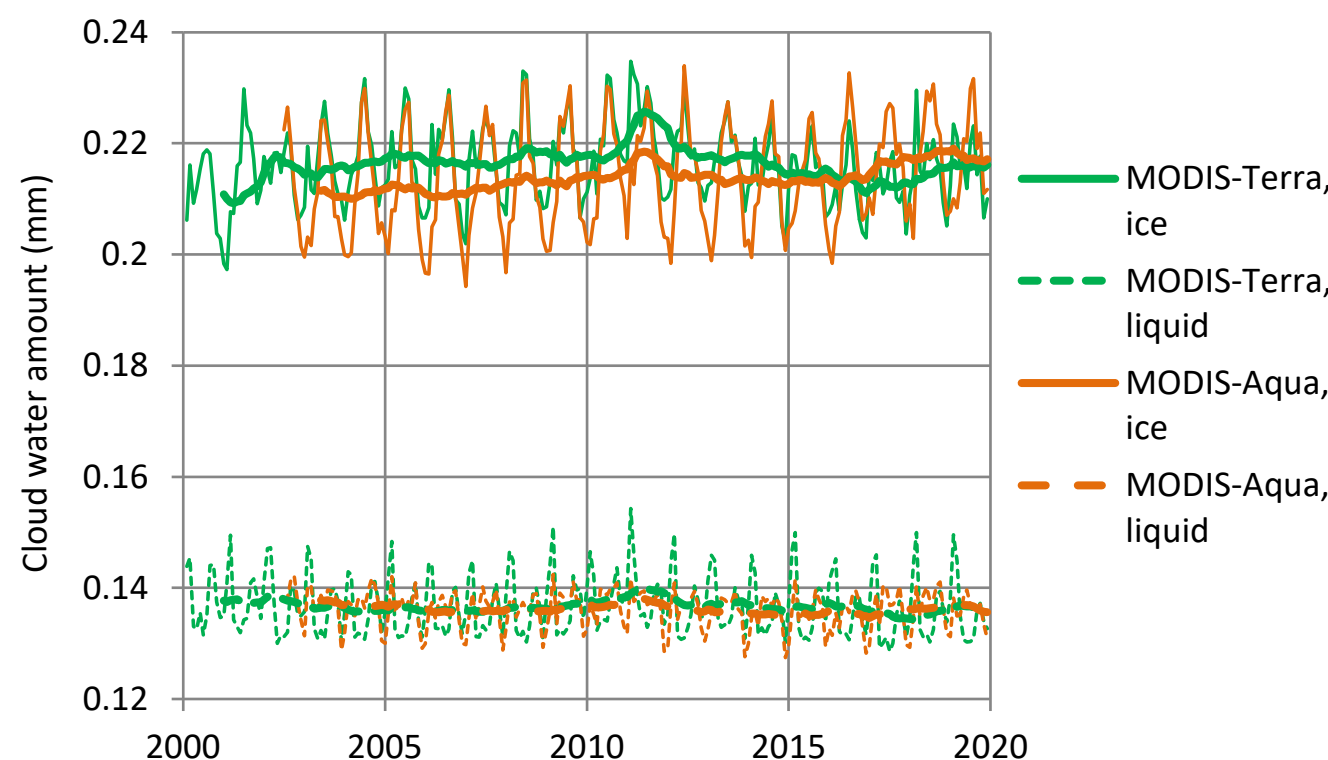
Figure 9: Variation of cloud water amount (in ice and liquid phase). Thin and thick lines of the same colour represent monthly values and running annual averages (right aligned), respectively. Sources of data are indicated in the legend and detailed in Table 1.
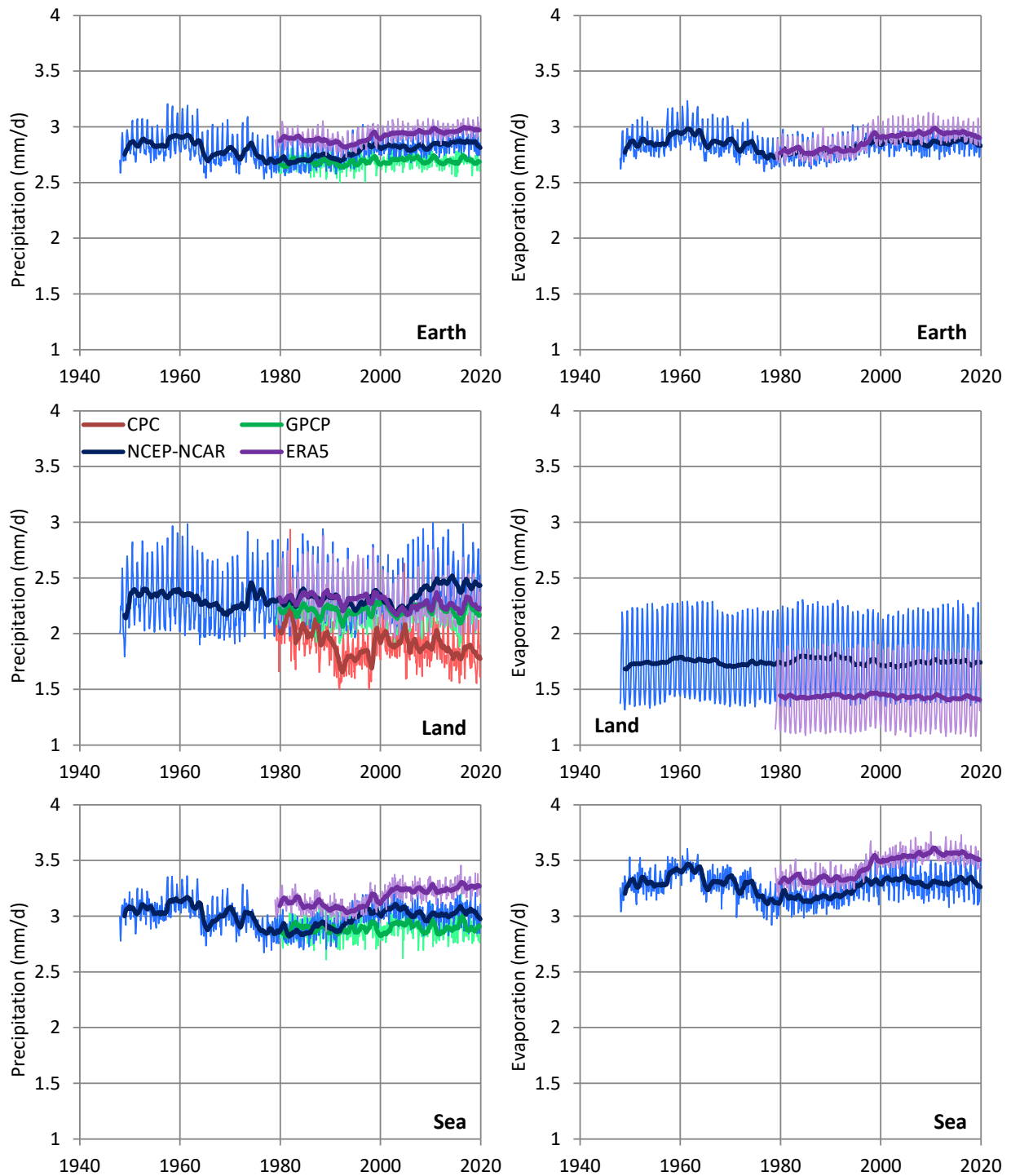
Figure 10: Variation of (left column) precipitation and (right column) evaporation. Thin and thick lines of the same colour represent monthly values and running annual averages (right aligned), respectively. Sources of data are indicated in the legend and detailed in Table 1; GPCP is version V2.3.

1140
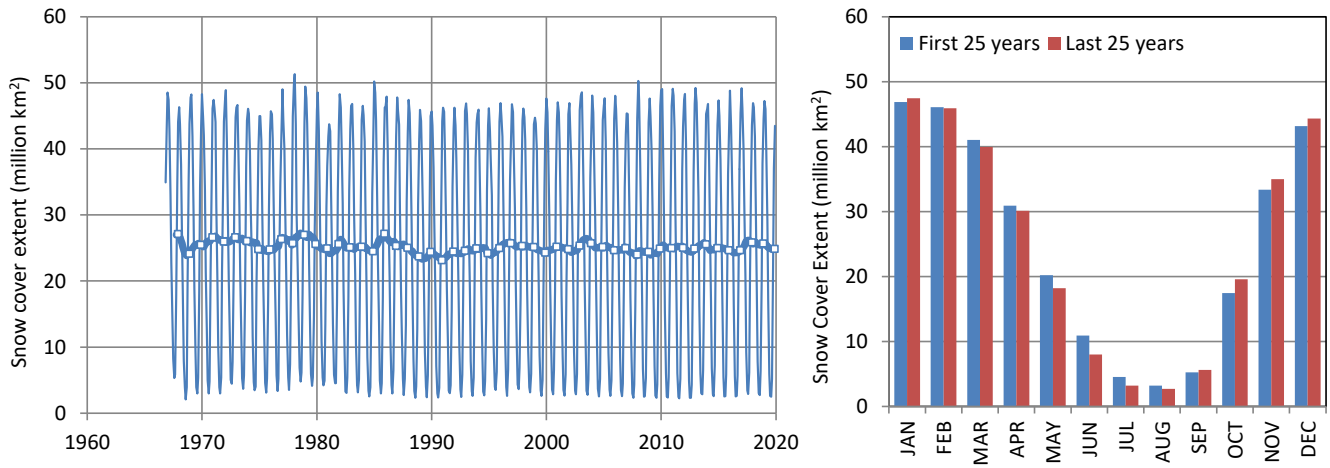
Figure 11: (Left) Variation of the snow cover extent in the northern hemisphere according to GSL; thin and thick lines represent monthly values and running annual averages (right aligned), respectively, and squares are annual averages aligned at December of each year. **(Right)** Seasonal variation of the snow cover, separately for the first and last 25 years of record.
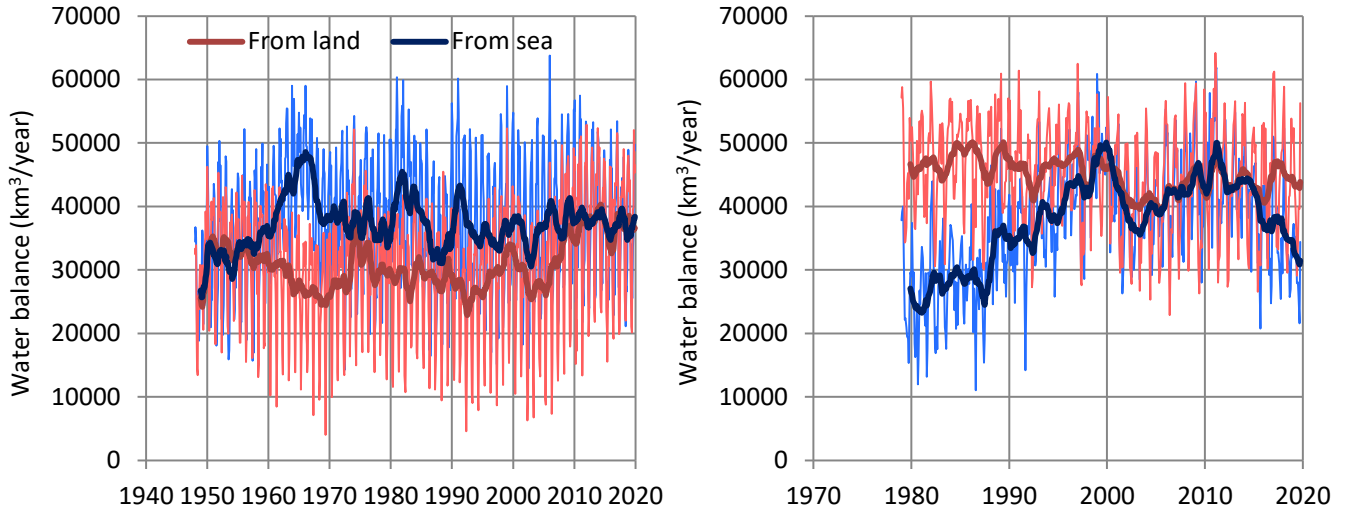
1145 **Figure 12:** Global water balance derived from the difference of precipitation and evaporation at land and sea from **(left)** the NCEP-NCAR and **(right)** the ERA5 reanalyses. Thin and thick lines of the same colour represent monthly values and running annual averages (right aligned), respectively.
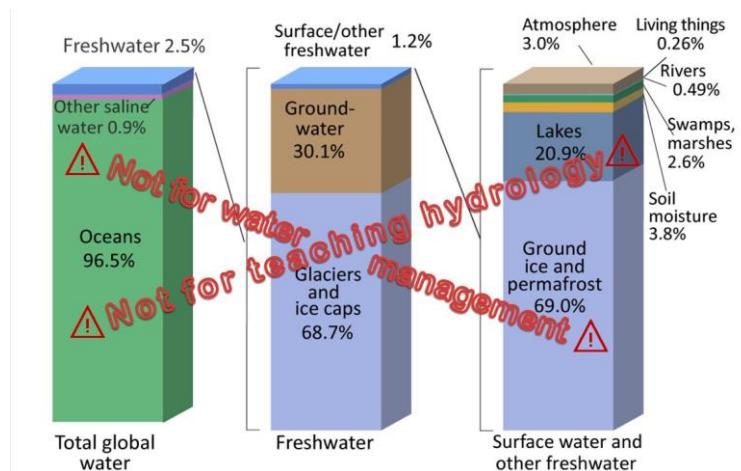
Figure 13: Typical depiction of water on Earth (source: USGS; https://www.usgs.gov/special-topic/water-science-school/science/oceans-and-seas-and-water-cycle and Wikipedia: https://en.wikipedia.org/wiki/Water_distribution_on_Earth#/media/File:Earth's_water_distribution.svg) with caution stamp added to discourage considering freshwater as non-renewable reserve.
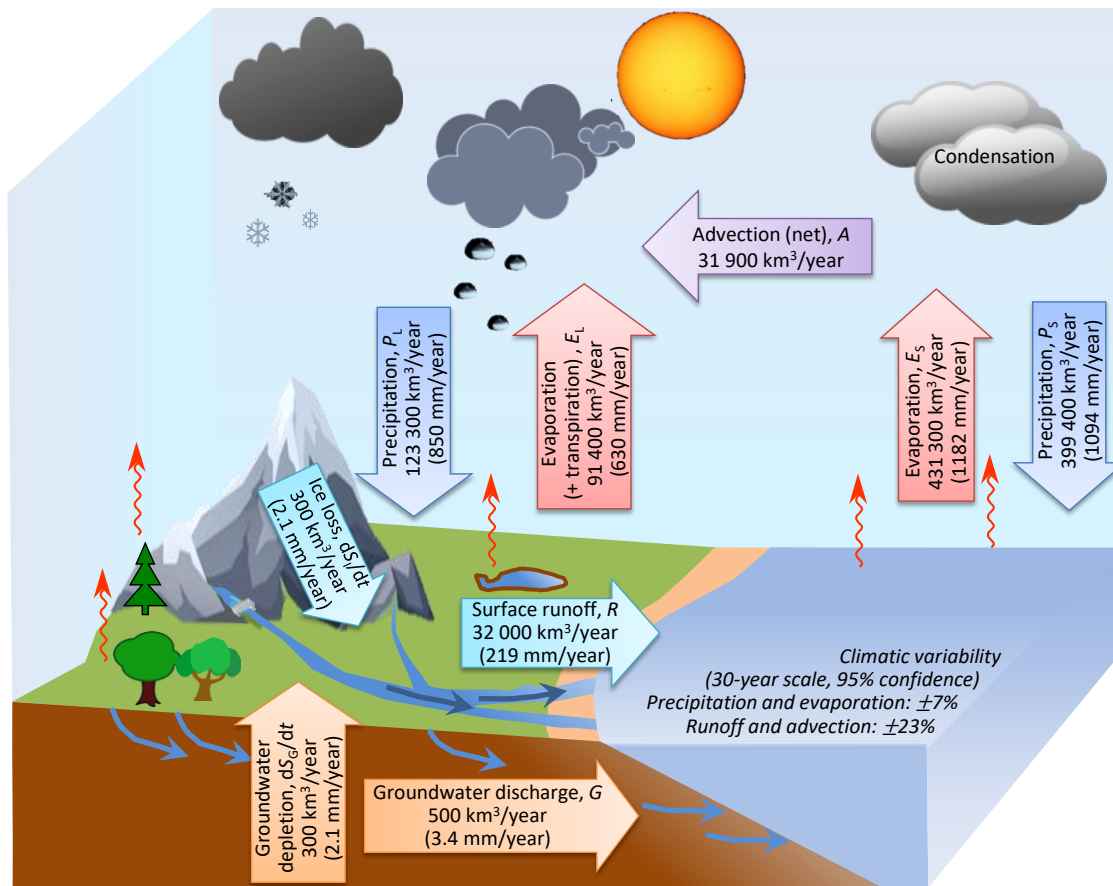
Figure 14: Proposed quantification of water balance.
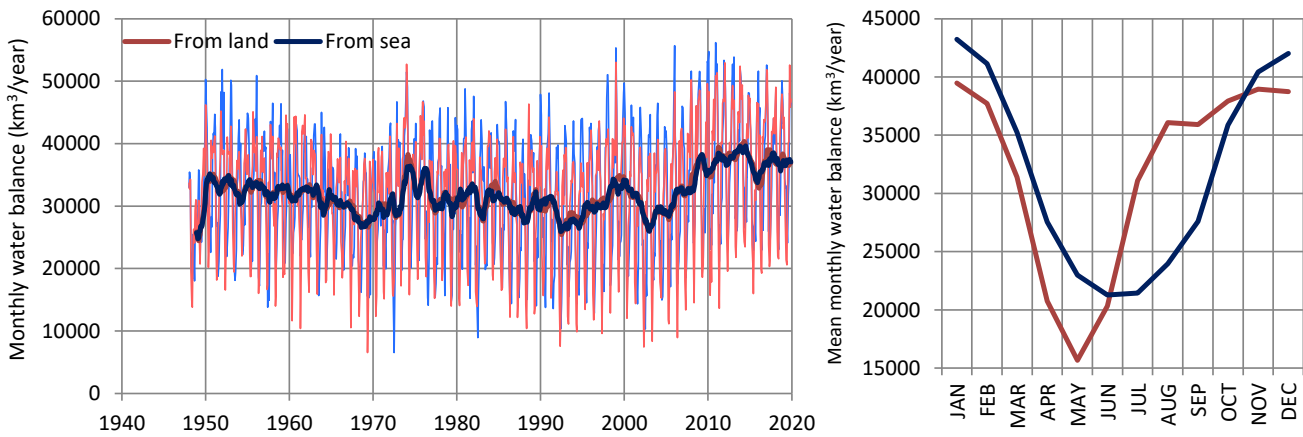
Figure 15: (Left) Final global water balance at land and sea from the NCEP-NCAR reanalysis. Thin and thick lines of the same colour represent monthly values (but with rates expressed in km³/year) and running annual averages (right aligned), respectively. (Right) Average seasonal variation of water balance.
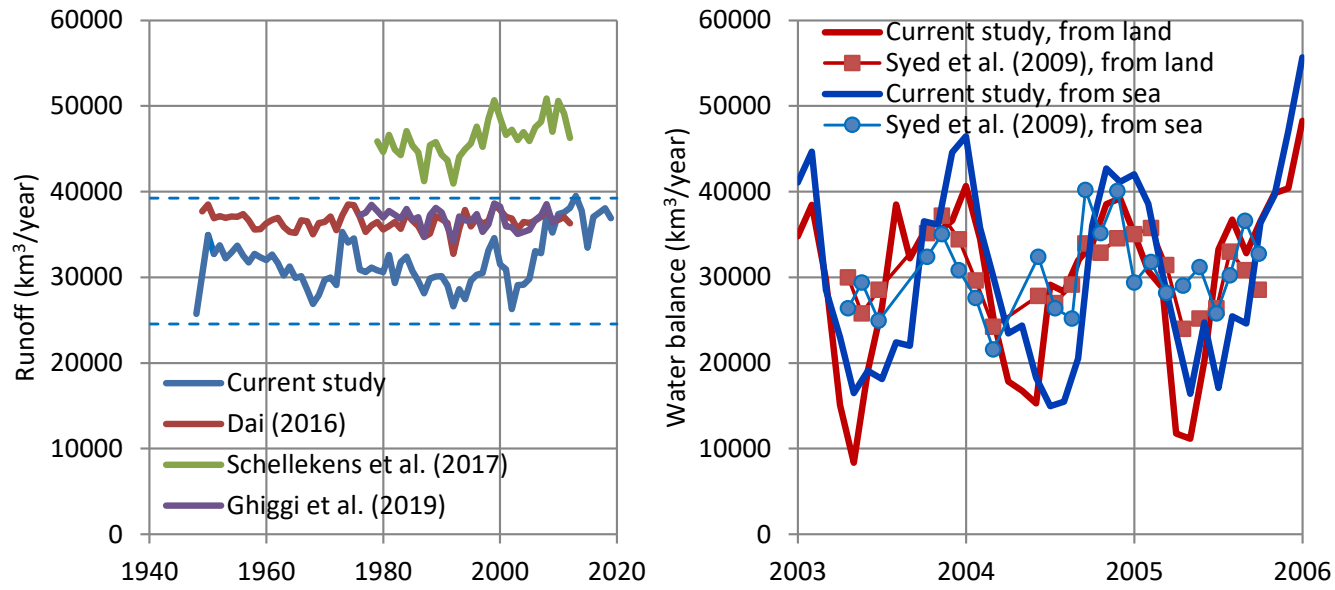
Figure 16: Comparison of results of the current study for surface runoff with those of (left) Dai (2016, Figure 2.8 digitized), Schellekens et al. (2017, Figure 7 digitized, ensemble mean) and Ghiggi et al. (2019, Figure 8a digitized, ensemble mean) at the annual scale, and (right) Syed et al. (2009, Figure 7 digitized) at monthly scale (but with rates expressed in km³/year). Dashed lines in the left panel are 95% confidence limits of the 30-year climatic average of the current study.

1165
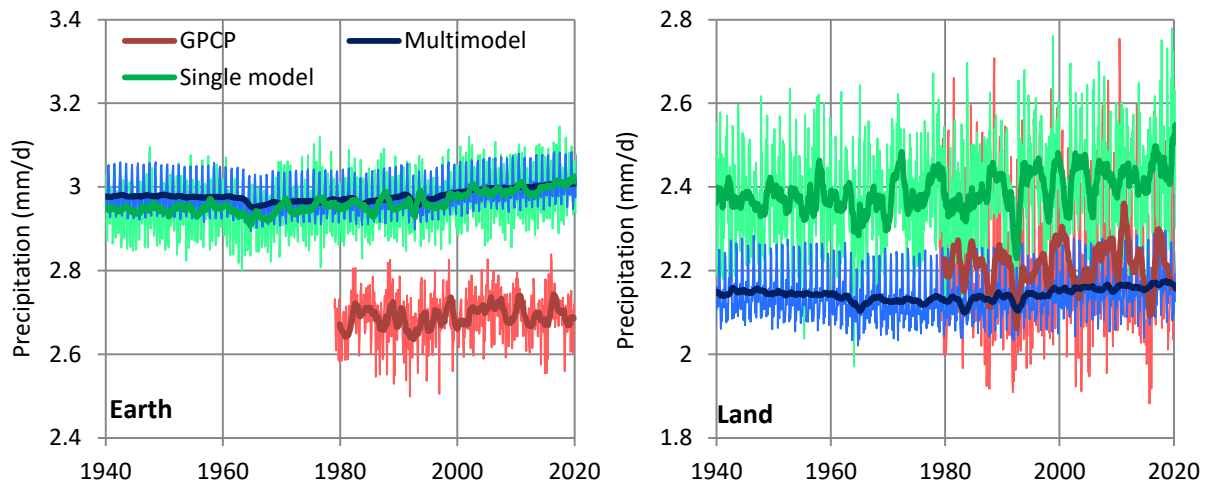
Figure 17: Comparison of climate model outputs (for specification of which see text) with reality, as quantified by GPCP satellite observations. "Multimodel" refers to CMIP5 scenario runs, entries: CMIP5 mean – rcp85. "Single model" refers to CCSM4 – rcp85, ensemble member 0, where CCSM4 stands for Community Climate System Model version 4, released by NCAR. Thin and thick lines of the same colour represent monthly values (but with rates expressed in km³/year) and running annual averages (right aligned), respectively.

1170
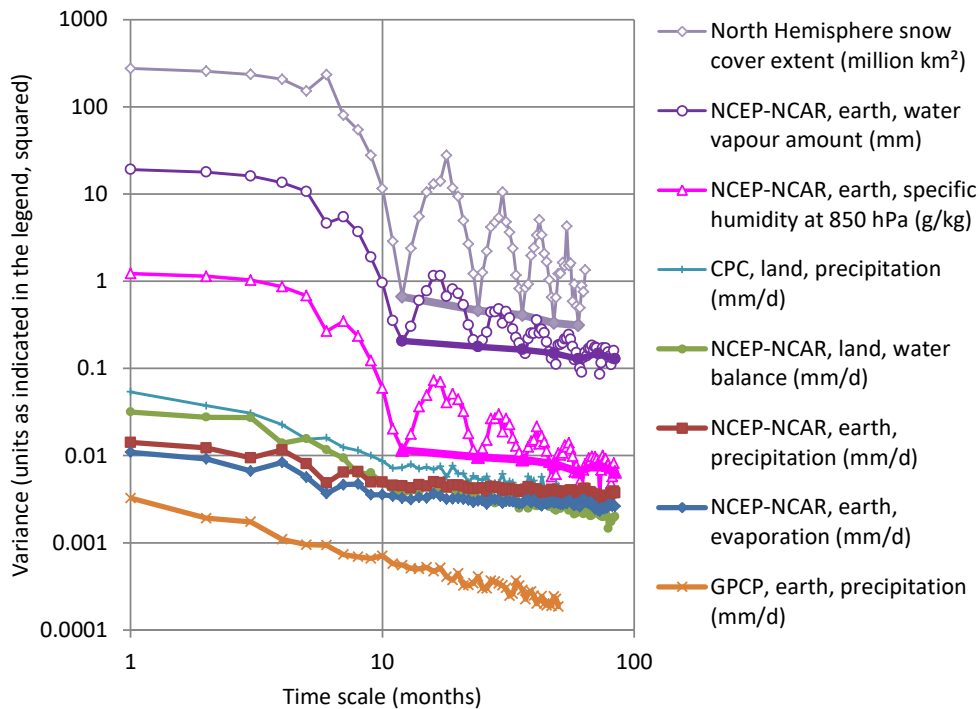
Figure 18: Climacograms of the indicated processes calculated from monthly time series; for some series with prominent seasonality the climacograms from annual time series are also plotted with thicker lines of same colour. For time scales larger than annually all slopes in the double logarithmic plots are close to –0.2, suggesting a Hurst parameter 0.90 (or larger if bias is taken into account). Exceptions are the NH snow cover extent with a slope of –0.47, suggesting a Hurst parameter 0.76 and the GPCP precipitation series

1175

with a slope of –0.72, suggesting a Hurst parameter 0.64.
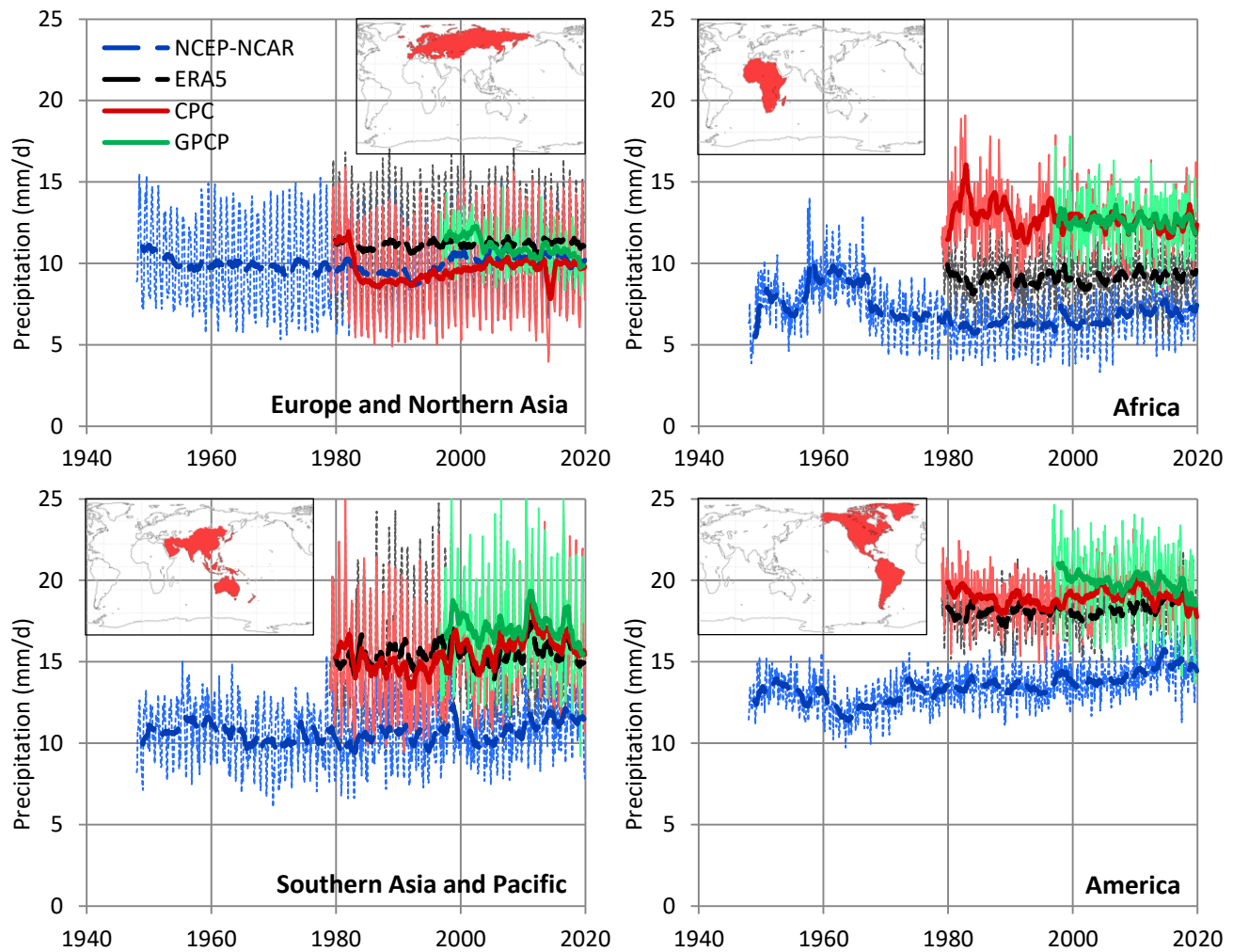
Figure B1: Variation of the monthly maximum daily precipitation areally averaged over the continents. Thin and thick lines of the same colour represent monthly values and running annual averages (right aligned), respectively. Dashed lines are for reanalyses and continuous lines for observations. Sources of data are indicated in the legend and detailed in Table 1.

1180
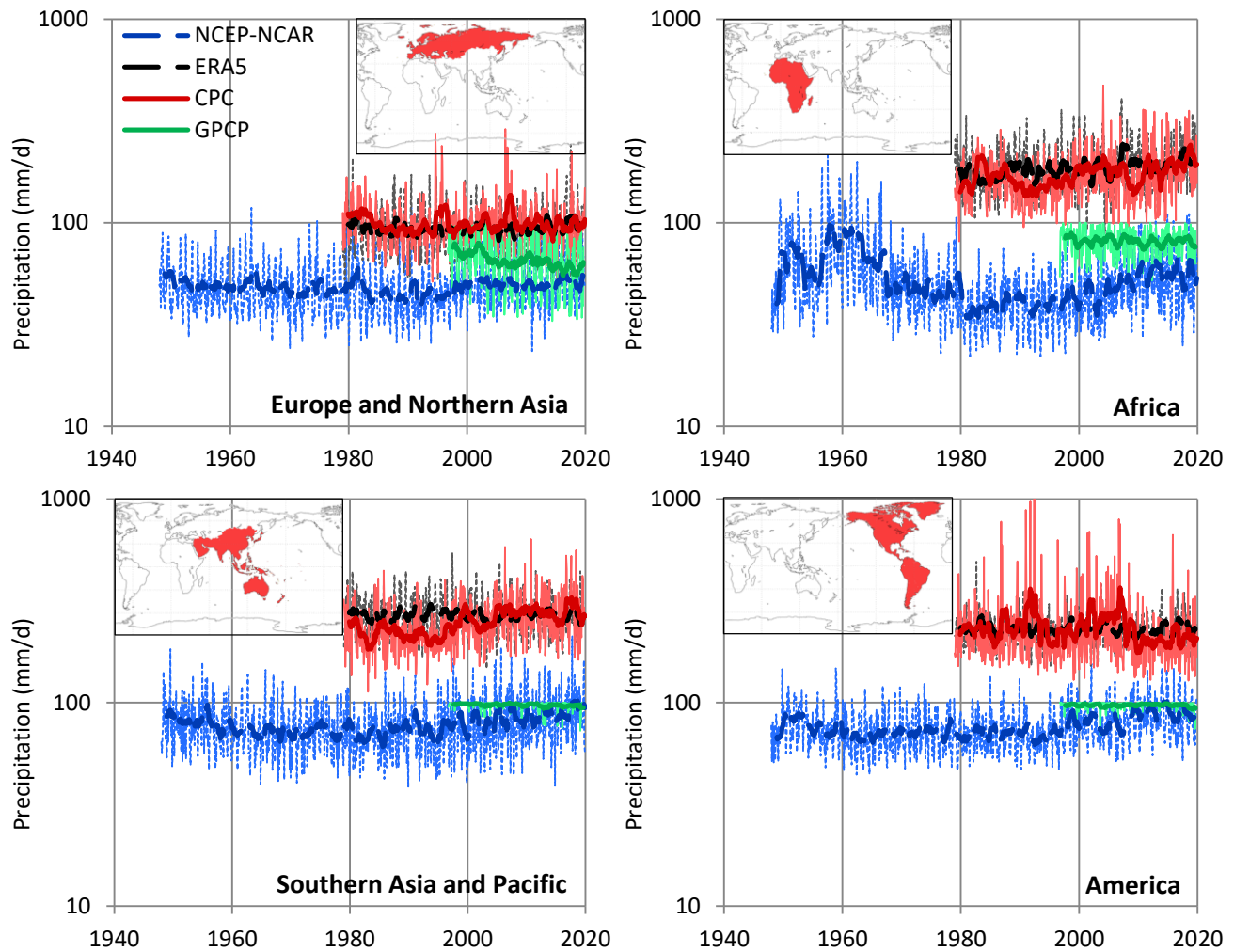
Figure B2: Variation of the areally maximum, over each continent, monthly maximum daily precipitation. Thin and thick lines of the same colour represent monthly values and running annual averages (right aligned), respectively. Dashed lines are for reanalyses and continuous lines for observations. Sources of data are indicated in the legend and detailed in Table 1. Notice that the satellite (GPCP) data do not seem to capture precipitation rates higher than 100 mm/d.
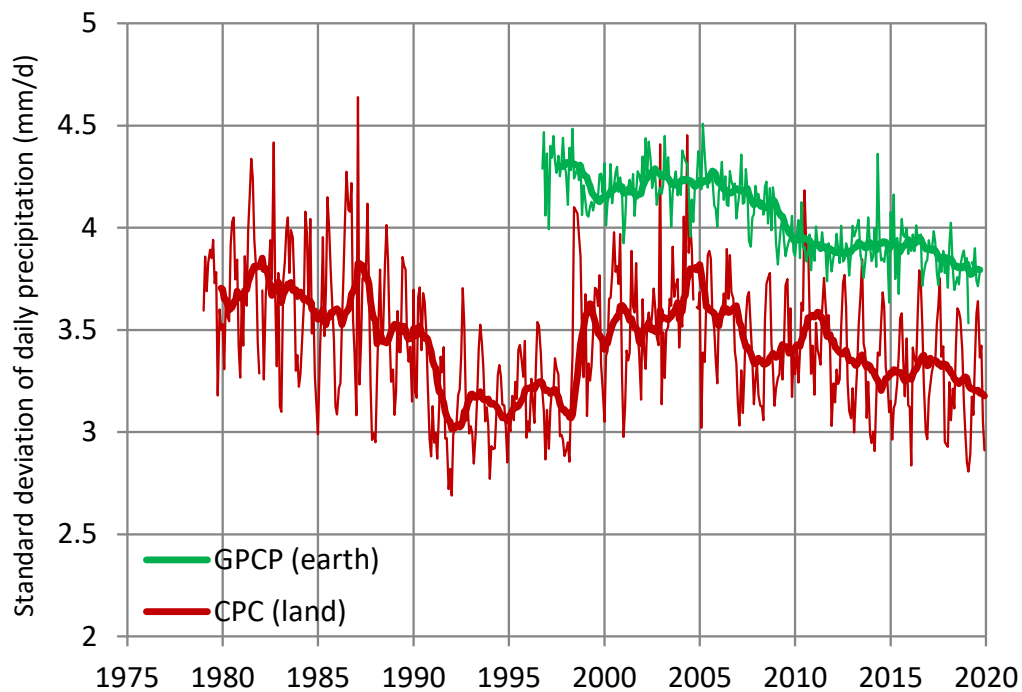
1185

Figure B3: Variation of the standard deviation of daily precipitation in each month, areally averaged. Thin and thick lines of the same colour represent monthly values and running annual averages (right aligned), respectively. Sources of data are indicated in the legend and detailed in Table 1.
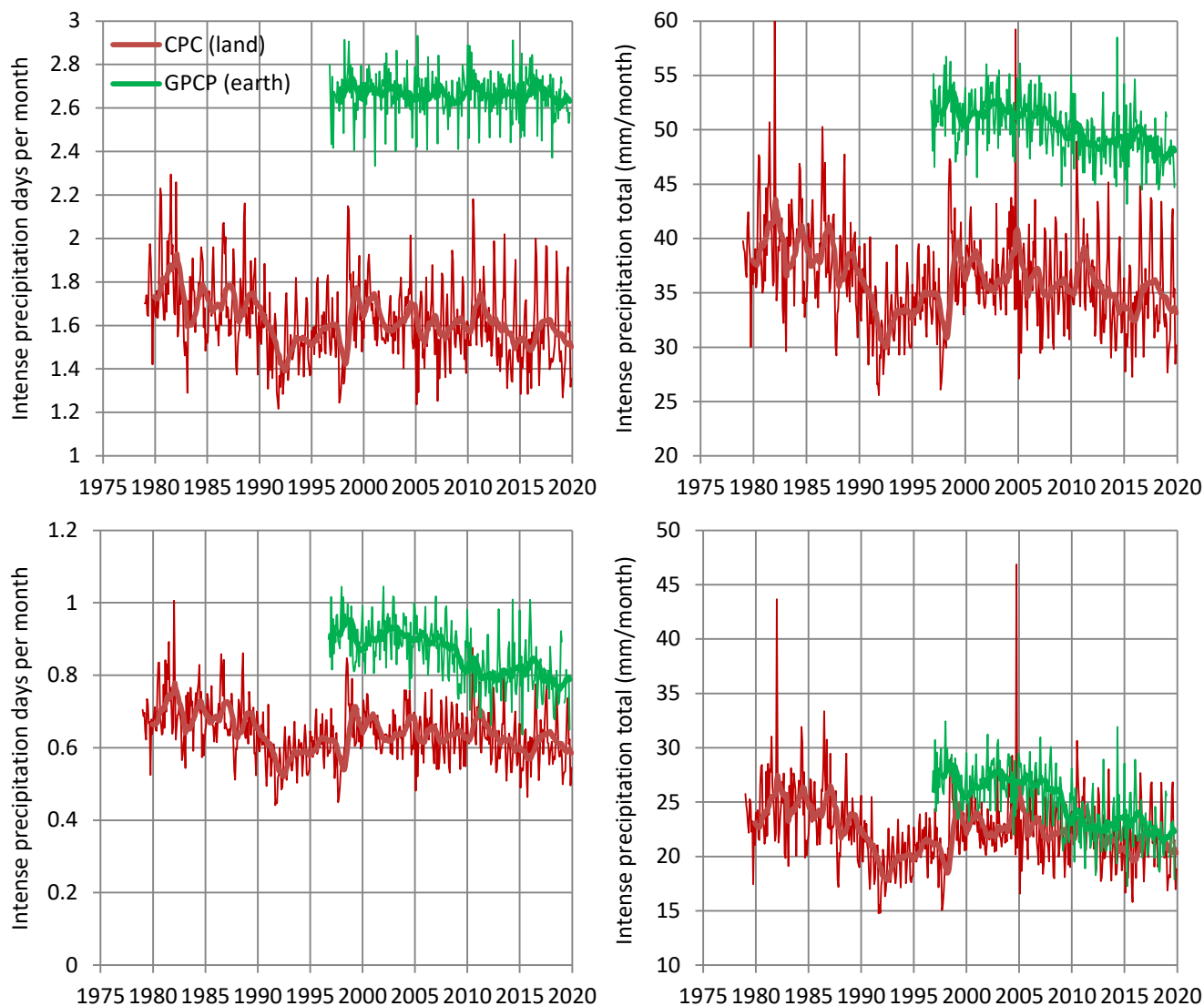
1190 **Figure B4: (Left column) Average days per month with precipitation exceeding a threshold value, which is 10 mm/d for the upper row and 20 mm/d for the lower row; (right column) monthly total of daily precipitation exceeding the threshold value. Thin and thick lines of the same colour represent monthly values and running annual averages (right aligned), respectively. Sources of data are indicated in the legend and detailed in Table 1.**
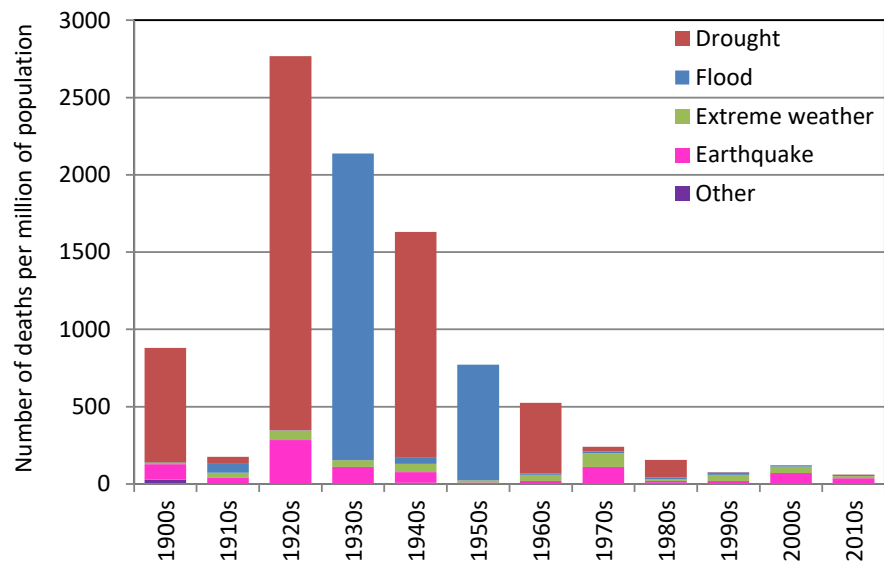
1195 **Figure B5: Evolution of the frequency of deaths from floods and droughts per decade of the 20th and 21st century. For comparison the deaths from other categories of natural catastrophes are also plotted: "Extreme weather" includes storm, extreme temperature (cold or heat wave, severe winter conditions) and fog; "Earthquake" also includes tsunami; "Other" comprises landslides (wet or dry), rock fall, volcanic activity (ash fall, lahar, pyroclastic flow, lava flow) and wildfire. For the sources of data see Table 1, entry 23.**

 Tables

Table 1: List and details of variables and data sets used in the study

# Variable, notation, unit, source acronym	Time scale, data type, time span	Description and original source	Additional sites for data access and processing
1 Temperature, T (°C) [UAH]	monthly, observations, 1978-2019	UAH temperature for the lower troposphere (global average) from satellite data, (http://www.nsstc.uah.edu/data/msu/v6.0/tlt/uahncdc_lt_6.0.txt)[*]	climexp (http://climexp.knmi.nl/), section: monthly observations
2 Temperature, T (°C)) [MODIS]	monthly, observations, Terra: 2000-2019 Aqua: 2002-2019	MODIS-Terra & MODIS-Aqua satellites (https://giovanni.gsfc.nasa.gov/giovanni/); observations from the Terra platform (MOD11C3 v006) are used	
3 Temperature, T (°C) [NCEP-NCAR]	daily & monthly, reanalysis, 1948-2019	NCEP-NCAR reanalysis (https://www.esrl.noaa.gov/psd/cgi-bin/data/testdap/timeseries.pl); resolution 1.88°; levels used for study: 2 m, 1000, 925, 850, 700, 600, 500, 400, 300 hPa	climexp, sections daily fields & monthly reanalysis fields
4 Temperature, T (°C) [ERA5]	daily & monthly, reanalysis, 1979-2019	ERA5 reanalysis by ECMWF (http://www.ecmwf.int/en/research/climate-reanalysis); resolution 0.5°; levels used for study: 2 m, 1000, 925, 850, 700, 600, 500, 400, 300 hPa	climexp, sections daily fields & monthly reanalysis fields
5 Dew point, T_d (°C) [ERA5]	daily, reanalysis, 1979-2019	As in 4 but only for the surface level	climexp, section daily fields[†]
6 Relative humidity, U (-) [NCEP-NCAR]	monthly, reanalysis, 1948-2019	As in 3	
7 Relative humidity, U (-) [ERA5]	monthly, reanalysis, 1979-2019	As in 4	
8 Specific humidity, q (g/kg) [NCEP-NCAR]	monthly, reanalysis, 1948-2019	As in 3; used levels for study: 850 hPa, 300 hPa	As in 3
9 Specific humidity, q (g/kg) [ERA5]	monthly, reanalysis, 1979-2019	As in 4; used levels for study: 850 hPa, 300 hPa	As in 4
10 Water vapour amount, W (mm) [NVAP]	monthly, observations, 1988-2009	NVAP, from the NASA Pathfinder project (http://nvap.stcnet.com/, section sample results, last figure)	Vonder Haar et al. (2012) (Figure 4c, after digitization)
11 Water vapour amount, W (mm) [MODIS]	monthly, observations, Terra: 2000-2019 Aqua: 2002-2019	MODIS-Terra & MODIS-Aqua satellites (https://giovanni.gsfc.nasa.gov/giovanni/); observations from both Terra (MOD08_M3) and Aqua (MYD08_M3) platforms are used	
12 Water vapour amount, W (mm) [NCEP-NCAR]	monthly, reanalysis, 1948-2019	As in 3	As in 3
13 Water vapour amount, W (mm) [ERA5]	monthly, reanalysis, 1979-2019	As in 4	As in 4

# Variable, notation, unit, source acronym	Time scale, data type, time span	Description and original source	Additional sites for data access and processing
14 Cloud water amount, W_{CI}, W_{CL} (mm) [MODIS]	monthly, observations, Terra: 2000-2019 Aqua: 2002-2019	As is 10	
15 Precipitation, P (mm/d) [CPC]	daily & monthly, observations, 1979-2019	CPC unified gauge-based daily precipitation gridded over land (https://www.cpc.ncep.noaa.gov/products/Global_Monsoons/gl_obs.shtml; https://climatedataguide.ucar.edu/climate-data/cpc-unified-gauge-based-analysis-global-daily-precipitation); resolution 0.5°	climexp, section daily fields (the first version, referring to the entire land grid —not only to grid boxes with observations)
16 Precipitation, P (mm/d) [GPCP]	daily & monthly, observations, daily (V1.3) 1996-2019; monthly: 1979-2019	GPCP precipitation data set combining gauge and satellite precipitation data over a global grid (https://www.ncdc.noaa.gov/cdr/atmospheric/precipitation-gpcp-daily – resolution 1°; https://www.ncdc.noaa.gov/cdr/atmospheric/precipitation-gpcp-monthly – resolution 2.5°).	climexp (both daily and monthly); NOAA-PSD (https://www.esrl.noaa.gov/psd/cgi-bin/data/testdap/timeseries.pl; monthly only)
17 Precipitation, P (mm/d) [NCEP-NCAR]	daily & monthly, reanalysis, 1948-2019	As in 3	As in 3
18 Precipitation, P (mm/d) [ERA5]	daily & monthly, reanalysis, 1979-2019	As in 3	As in 4
19 Snow cover extent S (km^2) [GSL]	monthly, observations for the Northern Hemisphere, 1967-2019	Snow cover by the Global Snow Laboratory (GSL) (https://climate.rutgers.edu/snowcover/table_area.php?ui_set=1&ui_sort=0); resolution: 88×88 grid points	NOAA's National Centers for Environmental Information (https://www.ncdc.noaa.gov/snow-and-ice/extent/snow-cover/nhland/0)
20 Evaporation, E (mm/d) [NCEP-NCAR]	monthly, reanalysis, 1948-2019	As in 3	As in 3
21 Evaporation, E (mm/d) [ERA5]	monthly, reanalysis, 1979-2019	As in 4	As in 4
22 Population (-)	annual, measurements, 1900-2019	United States Census (https://www.census.gov/data-tools/demo/idb/informationGateway.php)	Our World in Data (https://ourworldindata.org/world-population-growth)
23 Disasters (number of victims per disaster type) (-)	annual, measurements, 1900-2019	The OFDA/CRED International Disaster Database (Université Catholique de Louvain, Brussels, Belgium; OFRA stands for Office of U.S. Foreign Disaster Assistance; CRED stands for Centre for Research on the Epidemiology of Disasters, Belgium) (https://www.emdat.be)	Our World in Data (https://ourworldindata.org/ofdacred-international-disaster-data)

[*] The data set is given as "anomalies", which to convert to actual temperatures we used the monthly averages from http://www.drroyspencer.com/2016/03/uah-v6-lt-global-temperatures-with-annual-cycle/.

[†] For the NCEP-NCAR daily and monthly reanalysis neither the dew point nor the relative humidity at the surface level are available.

Table 2: Average air temperature (T) and dew point (T_d) in °C per 20-year and 10-year climatic periods, and resulting differences. Data from ERA5 reanalysis except for lower troposphere which is from UAH.

Variable and domain	First 20 years	Last 20 years	Difference in 20 years (and per decade)	First 10 years	Last 10 years	Difference in 30 years (and per decade)	Offset distance, km/decade[*] (offset height, m/decade[†])
T, earth	14.09	14.46	0.38 (0.19)	14.02	14.58	0.56 (0.19)	31 (29)
T, land	8.70	9.32	0.61 (0.31)	8.59	9.47	0.88 (0.29)	(45)
T, sea	16.21	16.49	0.28 (0.14)	16.16	16.59	0.42 (0.14)	(22)
T, lower troposphere	−9.27	−9.02	0.25 (0.12)	−9.34	−8.94	0.39 (0.13)	21 (20)
T_d, earth	9.17	9.38	0.21 (0.11)	9.13	9.47	0.34 (0.11)	21
T_d, land	0.86	1.14	0.28 (0.14)	0.75	1.22	0.47 (0.16)	
T_d, sea	12.48	12.66	0.18 (0.09)	12.46	12.76	0.29 (0.10)	

[*] The distance, which moving poleward in the temperate zone, would offset, on the average, the decadal increase of temperature or dew point.

[†] The height, which moving up would offset the decadal increase of temperature (assuming lapse rate of 6.5 °C/km).

Table 3: Average saturation vapour pressures, $e(T)$ and $e(T_d)$, in hPa per 20-year climatic periods and resulting differences. Data from ERA5 reanalysis.

	First 20 years[*]	Last 20 years[*]	Difference	% difference
$e(T)$, earth	16.14	16.54	0.40	2.4
$e(T)$, land	11.66	12.15	0.49	4.2
$e(T)$, sea	18.45	18.77	0.33	1.8
$e(T_d)$, earth	11.66	11.82	0.17	1.4
$e(T_d)$, land	6.70	6.83	0.13	2.0
$e(T_d)$, sea	14.48	14.66	0.18	1.2

[*] The values of $e(T)$ and $e(T_d)$ were estimated for each time step (month) and then averaged over the indicated period..

Table 4: Specific humidity at 850 hPa (q_{850}) and at 300 hPa (q_{300}) in g/kg per 30-year climatic periods, and resulting differences. Data from NCEP-NCAR reanalysis.

	First 30 years	Last 30 years	Difference	% difference
q_{850}, earth	6.13	6.14	0.02	0.4
q_{850}, land	5.47	5.43	–0.04	–8.1
q_{850}, sea	6.56	6.63	0.07	1.0
q_{300}, earth	0.271	0.255	–0.016	–6.0
q_{300}, land	0.232	0.204	–0.027	–12.5
q_{300}, sea	0.287	0.276	–0.011	–3.9

1215

Table 5: Water vapour amount (W) in mm per 30-year climatic periods, and resulting differences. Data from NCEP-NCAR reanalysis.

	First 30 years	Last 30 years	Difference	% difference
W, earth	25.15	25.11	–0.03	–0.1
W, land	18.04	17.66	–0.28	–1.5
W, sea	29.86	29.99	0.13	0.4

Table 6: Sensitivity analysis of water balance calculations.

Assumption for calculation	Resulting runoff, R (km³/year)
Adjustment of sea evaporation only	30 800
Proportional adjustment in both land and sea	32 000
Adjustment of land evaporation only	37 300

1220